Article:
Živná, M, Kidd, K, Zaidan, M et al. (2020) An international cohort study of autosomal dominant tubulointerstitial kidney disease due to REN mutations identifies distinct clinical subtypes. Kidney International, 98 (6). pp. 1589-1604. ISSN: 0085-2538

https://doi.org/10.1016/j.kint.2020.06.041

An International Cohort Study of Autosomal Dominant Kidney Disease due to *REN* Mutations Identifies Distinct Subtypes

Martina Živná, PhD[1], Kendrah Kidd, MS[1, 2], Mohamad Zaidan, MD, PhD[3], Petr Vyleťal, PhD[1], Veronika Barešová, PhD[1], Kateřina Hodaňová, PhD[1], Jana Sovová[1], Hana Hartmannová, PhD[1], Miroslav Votruba[1], Helena Trešlová[1], Ivana Jedličková [1], Jakub Sikora [1], Helena Hůlková [1], Victoria Robins[2], Aleš Hnízda[4], Jan Živný, PhD[5], Gregory Papagregoriou, PhD[6], Laurent Mesnard, MD[7], Bodo B. Beck [8,9], Andrea Wenzel, PhD[8,9], Kálmán Tory, MD, PhD[10,11], Karsten Häeffner, MD[12], Matthias T.F. Wolf, MD[13], Michael E. Bleyer, BS[2], John A. Sayer, MD PhD[14-16], Albert C. M. Ong, DM[17], Lídia Balogh, MD, PhD[11], Anna Jakubowska, MD[18], Agnieszka Łaszkiewicz, PhD[19], Rhian Clissold, MB ChB, MD[20], Charles Shaw-Smith, MD[20], Raj Munshi, MD[21,22], Robert M. Haws, MD[23], Claudia Izzi, MD[24], Irene Capelli, MD[25], Marisa Santostefano, MD[26], Claudio Graziano, MD[27], Francesco Scolari, MD, PhD[24], Amy Sussman, MD[28], Howard Trachtman, MD[29], Stephane Decramer, MD, PhD[30,31], Marie Matignon, MD[32,33], Philippe Grimbert, MD[32-34], Lawrence R. Shoemaker, MD[35], , Christoforos Stavrou, MD[36], Mayssa Abdelwahed, PhD[37], Neila Belghith, MD[37,38], Matthew Sinclair, MD[39,40], Kathleen Claes, MD, PhD[41,42], Tal Kopel, MD[43], Sharon Moe, MD[44], Constantinos Deltas, PharmR, PhD[6], Bertrand Knebelmann, MD, PhD[45-47], Luca Rampoldi, PhD[48], Stanislav Kmoch, PhD[1, 2], Anthony J. Bleyer, MD, MS[1,2]

[1]Research Unit of Rare Diseases, Department of Pediatric and Adolescent Medicine, First Faculty of Medicine, Charles University, Prague, Czech Republic; [2]Section on Nephrology, Wake Forest School of Medicine, Winston-Salem, NC, USA; [3]Service de Néphrologie-Transplantation, Hôpital de Bicêtre, Le Kremlin Bicêtre, France; [4] Department of Biochemistry, University of Cambridge, CB2 1TN Cambridge, UK; [5]Institute of Pathophysiology, First Faculty of Medicine, Charles University, Prague, Czech Republic; [6]Center of Excellence in Biobanking and Biomedical Research, Molecular Medicine Research Center, University of Cyprus, Nicosia, Cyprus; [7] Sorbonne Université, Urgences

Néphrologiques et Transplantation Rénale, Assistance Publique-Hôpitaux de Paris (APHP), Hôpital Tenon, Paris, France; [8]University of Cologne, Faculty of Medicine and University Hospital Cologne, Institute of Human Genetics, Cologne, Germany; [9]University of Cologne, Faculty of Medicine and University Hospital Cologne, Center for Molecular Medicine Cologne (CMMC) and Center for Rare Diseases Cologneies(ZSEK), Cologne, Germany; [10]MTA-SE Lendület Nephrogenetic Laboratory, Budapest, Hungary; [11]I[st] Department of Pediatrics, Semmelweis University, Budapest, Hungary;

[12]Department of General Pediatrics, Adolescent Medicine and Neonatology, Medical Center, Faculty of Medicine, Universitätsklinikum Freiburg, Freiburg, Germany; [13]Pediatric Nephrology, University of Texas Southwestern Medical Center, Dallas, TX, USA; [14]Renal Services, The Newcastle Hospitals NHS Foundation Trust, Newcastle upon Tyne, United Kingdom; [15]Translational and Clinical Research Institute, Faculty of Medical Sciences, Newcastle University, Central Parkway, Newcastle upon Tyne, United Kingdom; [16]NIHR Newcastle Biomedical Research Centre, Newcastle University, NE4 5PL, United Kingdom; [17]Kidney Genetics Group, Academic Nephrology Unit, Department of Infection, Immunity and Cardiovascular Disease, University of Sheffield Medical School, Sheffield, United Kingdom; [18]Department of Pediatric Nephrology Medical University Wroclaw, Poland;

[19]Laboratory of Molecular and Cellular Immunology, Hirszfeld Institute of Immunology and Experimental Therapy, Polish Academy of Sciences, Wroclaw, Poland; [20]Exeter Kidney Unit, Royal Devon and Exeter NHS Foundation Trust, Barrack Road, Exeter, Devon, United Kingdom;

[21]Division of Nephrology, Department of Pediatrics, Seattle Children's Hospital, Seattle, WA, USA;

[22]University of Washington, Seattle, WA, USA; [23]Pediatrics – Nephrology, Marshfield Medical Center, Marshfield, WI; [24]Division of Nephrology and Dialysis, Department of Medical and Surgical Specialties, Radiological Sciences, and Public Health, University of Brescia and Montichiari Hospital, Brescia, Italy; [25]Department of Experimental Diagnostic and Specialty Medicine (DIMES), Nephrology, Dialysis and Renal Transplant Unit, S. Orsola Hospital, University of Bologna, Bologna, Italy;

[26]Division of Nephrology, Ospedale Sant'Orsola-Malpighi, Bologna, Italy; [27]Medical Genetics Unit, Policlinico S. Orsola-Malpighi, Bologna Italy; [28]Department of Medicine, Division of Nephrology, University of Arizona Health Sciences Center, Tucson, AZ, USA; [29]Division of Nephrology, Department of Pediatrics, NYU School of Medicine, New York, NY, USA; [30]Pediatric Nephrology, CHU Purpan, Toulouse, France; [31]France Rare Renal Disease Reference Centre (SORARE), Toulouse, France;

[32]AP-HP (Assistance Publique-Hôpitaux de Paris), Nephrology and Renal Transplantation Department, Institut Francilien de Recherche en Néphrologie et Transplantation (IFRNT), Groupe Hospitalier Henri-Mondor/Albert-Chenevier, Créteil, France; [33]Université Paris-Est-Créteil, (UPEC), DHU (Département Hospitalo-Universitaire) VIC (Virus-Immunité-Cancer), IMRB (Institut Mondor de Recherche Biomédicale), Equipe 21, INSERM U 955, Créteil, France; [34]AP-HP (Assistance Publique-Hôpitaux de Paris), CIC-BT 504, Créteil, France; [35]Division of Nephrology, Department of Pediatrics, University of Florida, Gainesville, FL, USA; [36]Evangelismos Private Hospital, Pafos, Cyprus;

[37]Laboratory of Human Molecular Genetics, Faculty of Medicine, University of Sfax, Tunisia;

[38]Medical Genetics Department of Hedi Chaker Hospital, Sfax, Tunisia; [39]Division of Nephrology, Department of Medicine, Duke University School of Medicine, Durham, NC, USA; [40]Duke Clinical Research Institute, Durham, NC, USA; [41]Department of Nephrology and Renal Transplantation, University Hospitals Leuven, Belgium; [42]Laboratory of Nephrology, Department of Microbiology and Immunology, Katholieke Universiteit (KU) Leuven, Leuven, Belgium; [43]Nephrology Division, University of Montreal Hospital Centre, Hopital Saint-Luc, Montreal, Quebec, Canada; [44]Division of Nephrology, Indiana University School of Medicine, Indianapolis, IN, USA; [45]Department of Nephrology-Transplantation, Necker Hospital, APHP, Paris, France; [46]Paris Descartes University, Sorbonne Paris Cité, Paris, France; [47]Département Biologie cellulaire, INSERM U1151, Institut Necker Enfants Malades, Paris, France; [48]Molecular Genetics of Renal Disorders, Division of Genetics and Cell Biology, IRCCS San Raffaele Scientific Institute, Milan, Italy

Corresponding Author

Anthony J. Bleyer, MD, MS

Wake Forest School of Medicine

Section on Nephrology

Winston-Salem, NC, USA 27157

Fax: 336-716-4318

Phone: 336-716-4650

e-mail: ableyer@wakehealth.edu

RUNNING HEAD

Distinct subtypes of ADTKD-*REN* in an international cohort study

WORD COUNT: 4000

ABSTRACT

There have been few clinical or scientific reports of autosomal dominant tubulo-interstitial kidney disease due to *REN* mutations (ADTKD-*REN)*, limiting characterization. We formed an international cohort that characterized 111 individuals from 30 families both clinically and in the laboratory. Sixty-nine (62%) individuals had a *REN* mutation in the signal peptide region (signal group), 27 (24%) in the prosegment (prosegment group), and 15 (14%) in the mature renin peptide (mature group). Signal group patients were most severely affected, presenting at a mean age of 19.7±15.7 years, with the prosegment group presenting at 22.4±20.2 years, and the mature group at 37±12.4 years. Anemia was present in childhood in 91% in the signal group, 69% prosegment, and 0 of the mature group. *REN* signal peptide mutations reduced the signal peptide's hydrophobicity, which is necessary for recognition and translocation across the endoplasmic reticulum (ER) membrane, leading to aberrant delivery of preprorenin into the cytoplasm. *REN* mutations in the prorenin segment led to deposition of prorenin and renin in the endoplasmic reticulum Golgi intermediate compartment (ERGIC) and decreased prorenin secretion. Mutations in mature renin led to deposition of the mutant prorenin in the endoplasmic reticulum, similar to patients with ADTKD-*UMOD*, with a rate of progression to ESKD (63.6±7.6 y) that was significantly slower vs. the signal (50.8±17.6 y) and prosegment groups (53.1±10.6 years) (hazard ratio 0.367, p=0.023). Clinical and laboratory studies revealed subtypes of ADTKD-*REN* that are pathophysiologically, diagnostically, and clinically distinct.

KEY WORDS

Autosomal dominant tubulo-interstitial kidney disease, renin, mutation, characterization, signal peptide, prosegment,

INTRODUCTION

Autosomal dominant tubulo-interstitial kidney disease (ADTKD) is characterized by autosomal dominant inheritance, bland urinary sediment, and slowly progressive chronic kidney disease (CKD) leading to end-stage kidney disease (ESKD) between 30 and 80 years (1). While ADTKD was described in fewer than 10 families prior to 1990, genetic testing has led to increased detection, with over 300 families reported (2-5). ADTKD due to mutations in the *REN* gene encoding renin (ADTKD-*REN*) is one of the least common forms of ADTKD (5), with only 8 families and 28 individuals reported before 2020 (5-11).

Renin is a hormone primarily produced in the kidney that is requisite for tubulogenesis (12) and embryonic kidney formation (13). The renin angiotensin system (RAS) is a key modulator of blood pressure (14) and CKD progression (15). Renin biosynthesis constitutes the first enzymatic steps in the RAS. The human renin precursor is synthesized in the juxtaglomerular cells of the macula densa as a 406 amino acid preprorenin, composed of a 23 amino acid N-terminal signal peptide, a 43 amino acid prosegment, and a 340 amino acid mature renin peptide (16). During biosynthesis, the signal peptide mediates insertion of the nascent preprorenin into the translocation channel in the endoplasmic reticulum (ER) and initiates cotranslational translocation of preprorenin into the ER lumen, where glycosylation and proteolytic processing of the nascent preprorenin occur, conditioning further transit of prorenin and renin through the constitutive and regulated secretory pathways (17).

In ADTKD-*REN*, heterozygous *REN* mutations lead to decreased synthesis of prorenin and renin, resulting in mild hyperkalemia, anemia, hyperuricemia, and a predisposition to the development of acute kidney injury (5). *REN* mutations have been reported in the segment of the *REN* gene encoding the signal peptide (5-8) and the mature renin protein (9, 10). Mutations in the prosegment – a segment of the gene after the signal peptide that assists in protein folding – have not been reported. The small

number of case reports of ADTKD-*REN* has prevented clinical correlation with mutation type and identification of risk factors for progression to ESKD.

We performed an international retrospective cohort study and collected clinical and genetic data on 111 individuals from 30 families with heterozygous *REN* mutations in order to better characterize this condition. We performed laboratory investigations on ten representative mutations (five in the signal peptide, three in the prosegment, and two in mature renin) and characterized two missense *REN* variants of unknown significance found in African-Americans, p.P8A and p.R33W.

RESULTS

Of 111 individuals from 30 families (see Table 1 and Supplementary Figures S1, S2), sixty-nine (62%) individuals had a mutation in the signal peptide, 27 (24%) in the prosegment, and 15 (14%) in the mature renin peptide. A mutation in p.S45N was identified in one individual with ADTKD of unknown cause. This mutation did not segregate with disease and was determined to be nonpathogenic; it was included as a control for laboratory investigations. While searching variant databases, we noticed two additional rare missense variants (AA_*REN* variants) found specifically in African-Americans, a group with an increased prevalence of low-renin hypertension and CKD (18). These variants encode p.P8A in the signal peptide and p.R33W in the prosegment of preprorenin. Their allelic frequencies in African-Americans are 0.007 and 0.001 respectively.

Effect of Mutation Class on Clinical Characteristics

Presentation

After excluding patients with missing data (n=14) and those identified by genetic screening (n=16), there were 81 patients for analysis (see Table 2). Patients in the signal group were the most severely affected and presented at the youngest age. The mean age of clinical presentation was 19.7±15.7 years for the signal group, 22.4±20.2 years for the prosegment group, and 37.0±12.4 years for the mature group

(p<0.001 for comparison of the mature group vs. signal and prosegment group). Only patients in the signal group presented with acute kidney injury (10%) or acidosis, anemia, and kidney failure (13%). Thirty-one percent of patients in the signal group and 50% of patients in the prosegment group presented with anemia. Patients in the mature group presented only with gout (75%) or CKD (25%). The mean age of presentation was similar for men and women (19.3±13.7 years vs. 19.9±19.4 years, p=0.6).

Kidney function

Kidney function was less severely affected in the mature group vs. the signal and prosegment groups. Figure 1A displays all estimated glomerular filtration (eGFR) values obtained for the entire cohort of patients. An eGFR of 10 mL/min/1.73m^2 was assigned at the age of ESKD. Patients in the signal and prosegment group presented much earlier in life. At earliest clinical presentation, the majority of eGFR readings in these groups were below 60 mL/min/1.73 m^2, suggesting that decreased kidney function is present at birth in most patients. Despite early decreased function, eGFR values tended to remain relatively stable during childhood and through adolescence. Figure 1B shows data on 13 children in the signal group with multiple eGFR measurements. In almost all cases, eGFR remained steady with minimal decline, including one patient whose eGFR remained stable at approximately 30 mL/min/1.73m^2 from age 2 through age 16 (Figure 1B: p.C20R with red markers). Another patient (p.M39K) presented during infancy with an eGFR of 19 mL/min/1.73 m^2 and had a relatively stable eGFR through childhood before proceeding to renal replacement therapy at 15 years, being the only individual reaching ESKD prior to age 30 years. After adolescence, there was in general a slow decline in eGFR in the signal and prosegment groups (see Figure 1A). The median age of ESKD was 57 years in the signal group, 62 years in the prosegment group, and 68 years in the mature group (Figure 2). Patients in the mature group had no laboratory values until age 20 years, due to milder manifestations (see Figure 1A). Patients in the mature group presenting at this age appeared to have normal kidney function.

To evaluate risk factors for ESKD progression, univariate Cox proportional hazards models were created, with the event being age of ESKD. Patients in the mature group had a significantly decreased risk of developing ESKD over time vs the signal and prosegment groups combined, with a hazard ratio of 0.37 (p=0.023) (See Table 3 and Figure 2). In other univariate models, anemia in childhood (hazard ratio 2.82, p=0.03) (See Table 3 and Figure 3) was significantly associated with an earlier age of ESKD, while gender was not associated with progression to ESKD. The best-fit Cox proportional hazards model included only anemia in childhood (See Table 3 and Figure 3).

Anemia

Figure 4A shows hemoglobin levels in patients not on erythropoietin. The lowest hemoglobin values were 7.5 g/dL. The mean hemoglobin level was 9.6±1.04 g/dL for age <10 years, 10.1±1.1 g/dL for 10 to <15 years, and 10.5±1.2 g/dL for ages 15 to < 20y. Females were more likely to have anemia as a child (97% vs. 46%, p=0.005) and have lower hemoglobin levels (see Table 4 and Figure 4A). Hemoglobin levels in women tended to remain low over time, while in men, hemoglobin levels appeared to rise after age 20 years. For 14 children who never received erythropoietin, the mean hemoglobin level was 9.8±1.2 g/dL (range 7.4-13.8 g/dL). For children who received erythropoietin, while not receiving erythropoietin the mean hemoglobin level was 10.1±1.3 g/dL (range 7.6-12.6 g/dL).

Hyperkalemia and academia

Hyperkalemia was present but rarely reach life-threatening levels. Figure 4 shows serum potassium according to age (4B) and eGFR (4C). Serum bicarbonate levels vs. age are depicted in Figure 4D. Serum bicarbonate values were frequently below 24 mEq/L.

Gout

In individuals not taking allopurinol or febuxostat, males had a higher serum urate level than women (9.4±2.7 mg/dl vs. 7.7±1.6 mg/dl, p=0.02) and were more likely to have gout (49.3% vs. 39.5%, p<0.01).

Renin levels

Plasma renin levels were low, with the mean random plasma renin activity (normal range 2.9 to 24 ng/mL/h) in the signal group 0.5±0.8 ng/ml/h (n=18), in the prosegment group 0.5±0.6 ng/ml/h (n=4), and in the mature group 0.8±0.7 ng/ml/h (n=5).

Fludrocortisone

Fludrocortisone was administered to two patients consistently and in seven patients for a short period of time. There were no adverse effects from fludrocortisone. In one patient, it was taken consistently from age 11 onwards, and in another patient from age 13 (Figure 5). The serum potassium values were lower in nine individuals while taking vs. not taking fludrocortisone (4.37±0.54 mEq/L vs 4.77±0.55 mEq/L, $p< 0.01$). The serum bicarbonate values were also higher (25.9±2.3 mEq/L vs. 23.7±3.5 mEq/L, $p=0.003$).

***In silico* analysis**

Figure 6A displays the *REN* mutations identified in ADTKD families. Except for the p.T26I and the non-pathogenic p.S45N, all amino acid residues at mutation sites are absolutely conserved across species (**Figure 6B**). SignalP 4.1 prediction software (19) indicates that all signal peptide mutations except p.C20R decrease the cleavage site prediction scores (C-score) (**Figure 6C**), suggesting a decrease in the efficacy of the signal peptidase mediated release of the signal peptide from preprorenin. Scores for the AA_*REN* p.P8A variant are similar to wild type (**Figure 6C**).The mutations in the prosegment, including the AA_*REN* variant p.R33W, are classified by the M-CAP pathogenicity classifier (20) as either likely benign (p.T26I, p.M39K and p.S45N (non-pathogenic)) or possibly pathogenic (p.R33W). Mutations in mature renin (p.C325R, p.I366N) are classified as possibly pathogenic (**Figure 6D**).

All mutations have significant effects on prorenin structure (**Figure 7**) and may modulate renin activity by affecting the folding, constitutive secretion and proteolytic processing of prorenin (21-23).

Functional studies of identified *REN* variants

Wild type and mutant proteins were transiently expressed in HEK293 cells (**Figure 8**). Western blot and immuno-detection of corresponding proteins showed that the wild type protein was present in the cell lysate in three major forms (Figure 8A) corresponding to preprorenin (45 kDa), prorenin (47 kDa) and renin (43 kDa), with the preprorenin being less abundant. In the culture media (Figure 8B), only prorenin was detected. Proteins with mutations in the signal peptide were present in cell lysates mostly in the form of preprorenin, with no prorenin or renin detected in culture media. Proteins with mutations p.T26I and p.M39K in the prosegment were present in cell lysates in all three forms similar to the wild type protein, whereas the nonpathogenic p.S45N was present mostly in the form of prorenin. Prosegment mutations affected secretion of p.M39K prorenin into culture media; however, secretion of p.T26I and p.S45N was unaffected. Proteins with mutations in the mature renin were present in cell lysate predominantly as prorenin and were not secreted into culture media. Proteins with AA_*REN* variants in the signal peptide (p.P8A) or prosegment (p.R33W), showed similar profiles to wild type protein in cell lysates. The mutation p.R33W affected secretion of prorenin into culture media (**Figure 8A,B**). Quantitative immunoradiometric assay **(Figure 8E,F)** showed that mutations in the signal peptide either significantly reduced (p.L16del) or entirely prevented renin and prorenin synthesis in cells and their secretion into culture media. Mutations in the prosegment had either no effect or a marginal effect (p.M39K) on renin and prorenin synthesis, but affected secretion of p.T26I and p.M39K into culture media. Secretion of nonpathogenic p.S45N was unaffected. Mutations in the mature renin led to the synthesis of prorenin and renin that were either inactive or undetectable by the antibody used in the assay. The AA_*REN* variant p.P8A had no effect on renin and prorenin synthesis in cells and secretion of prorenin and renin into the culture media. For the AA_*REN* variant p.R33W, there was reduced secretion of prorenin into the culture media (**Figure 8C, D**). Proteolytic activity assay showed that mutations in the signal peptide either reduced (p.L16del) or entirely abolished renin activity in culture media. Mutations

in the prosegment led either to a production of proteolytically "hyperactive" prorenin (p.M39K) or reduced the activity of renin in the culture media (p.T26I, p.S45N). Mutations in the mature renin abolished production of active renin. The AA_*REN* variant p.P8A had no effect on the proteolytic activity of secreted renin and prorenin. The AA_*REN* variant p.R33W reduced renin activity via low prorenin secretion (**Figure 8E, F**). Mutated proteins had altered intracellular localization (**Figure 9A**). Wild type protein was present in coarsely granular structures that were localized in the cytoplasm and in the LAMP2 positive lysosomal-like structures. Proteins with signal peptide mutations demonstrated mostly diffuse cytoplasmic staining. Proteins with prosegment mutations were localized mainly to endoplasmic reticulum intermediate compartment (ERGIC). Proteins with mutations in the mature renin formed intracellular clumps localized in the ER **(Figures 9A,B, Supplementary Figure S3**). There was little renin staining in the Golgi apparatus for wild-type and *REN* mutations (**Supplementary Figure S4).** Wild type protein and proteins with prosegment mutations were localized in lysosomes whereas proteins with signal peptide mutations (except of p.L16del) and proteins with mutations in the mature renin were not (**Supplementary Figure S5**). All functional data are summarized in **Table 5.**

DISCUSSION

In this work we describe distinct clinical and pathophysiologic differences (**Figure 10**) in signal, prosegment, and mature peptide mutations of the *REN* gene in a cohort of 111 patients from 30 families with ADTKD-*REN*.

Patients with mutations in the signal peptide region were the most severely affected. One-third presented before age 10, with 10% having acute kidney injury and 13% presenting with anemia, acidosis, and kidney failure. The mean age of presentation was lower than in the other two groups (19.7±15.7 years vs. 22.4±20.2 years and 37.0±12.4 years). We demonstrated that transiently expressed proteins with mutations in the signal peptide lead to proteosynthesis of preprorenin that, according to

immunofluorescence studies, is probably located in the cytoplasm or faces the cytoplasmic side of the ER or ERGIC membranes. This phenomena has previously been described in a case of signal peptide mutations of preproinsulin leading to β cell failure and autosomal dominant diabetes (24, 25) and in a mutation in the preproparathyroid hormone (*PTH)* gene resulting in familial isolated hypoparathyroidism (26). The effects of aberrant renin production not only resulted in manifestations of clinical renin deficiency but likely also affected normal renal embryogenesis, resulting in decreased kidney function at birth. The presence of significantly decreased renin activity in the setting of a heterozygous mutation is likely due to the mutated protein blocking the translocon and affecting synthesis of functional renin from the wild-type allele, a phenomenon that has been observed in ADTKD caused by mutations of Translocon Subunit Alpha 1 (SEC61A1) (4) or in preproinsulin signal peptide mutations, resulting in permanent neonatal diabetes, despite the presence of a wild-type insulin allele (27).

61% of individuals in the prosegment group presented at less than 10 years (61%), often presenting with gout (36%) and anemia (50%). The prosegment (propeptide) is a structural element that determines the biosynthesis, cellular trafficking and function of most proteases (28), including prorenin (21-23). Mutations in the prosegment leading to dominant phenotypes have been reported in several other preproteins, including proinsulin (leading to diabetes) (29) and factor IX deficiency (haemophilia) (30). The prosegment mutations in prorenin described here are classified as likely benign by various pathogenicity prediction programmes. However, based on structural studies, they are predicted to change interactions of the prosegment region with renin that are critical for the maintenance of the protease in its inactive state [24]. Accordingly, we demonstrated that mutations in the prosegment do not significantly affect the amounts of synthesized prorenin and renin, but rather they alter secretion and enzyme activity regulating properties of the prosegment as demonstrated by altered proportions of synthesized, enzymatically active renin and prorenin (**Table 5**). This altered proportion may also reflect

the effect of prosegment mutations on trafficking through the intracellular vesicular network, within which processing of prorenin to renin occurs. Such an effect is suggested by specific accumulation of proteins with prosegment mutations (compared to other *REN* mutations) in the ER-Golgi intermediate compartment (ERGIC), where the quality control system of the early secretory pathway and the concentration process of nascent secretory proteins into secretory granules take place (31). The age of presentation and severity of prosegment mutations may vary significantly due to the type of mutation and its specific effects on biosynthesis, cellular trafficking and proteolytic processing of prorenin and renin activity regulation. In addition to causing cellular toxicity, these dominant negative effects may be due to abnormal interactions between the mutant and wild-type proteins that are being processed in parallel, as seen in early onset insulin-deficient diabetes (32). The non-pathogenic p.S45N variant showed normal *in vitro* scores and normal (actually increased) enzyme activity. Accumulation in the ERGIC however suggests that the p.S45N mutation affects protein trafficking and could potentially lead to late-onset CKD.

Mutations in the genetic region encoding the mature renin peptide had a much milder course compared to patients with mutations in the region encoding the signal peptide or preprorenin, as first noted by Schaeffer in a case report of a family with the p.L381P *REN* mutation (11). In contrast to patients in the signal and prosegment group who often present in childhood, patients in the mature group first present in their twenties with gout or present later in life with unexplained CKD. These patients appear to have normal kidney function early in life. Whether individuals in the mature group had anemia in childhood is unclear, but if present it was asymptomatic in the patients in our cohort. Two mutations in mature renin were studied *in vitro*. These mutations destabilize renin structure and produce an enzymatically inactive prorenin that is trapped within the ER, similar to the mature *REN* mutation p.L381P (11). The localization of the mutated mature renin protein and pathophysiologic changes are very similar to changes found in ADTKD due to *UMOD* mutations, and the two conditions

are quite similar clinically. Better clinical outcomes in the mature group may be due to decreased cellular toxicity of the mature renin mutations and decreased effects on cellular processing of the wild-type renin produced by the normal allele, similar to mutations in the mature insulin peptide found in diabetes mellitus, with onset of symptoms in adulthood (33-35).

REN mutations identified in African-Americans

We also evaluated two missense *REN* variants of unknown significance, p.P8A and p.R33W, which are located in the signal peptide and prosegment of preprorenin and are present in relatively high frequencies in African-Americans. Individuals of African descent show a higher prevalence of low renin hypertension and ESKD (18), and we were interested to evaluate their functional impact. Our analyses demonstrated that whereas the p.P8A variant has no effect, the p.R33W variant has altered properties that are very similar to other ADTKD-*REN* prosegment mutations. With population frequencies of 0.001 the p.R33W may thus represent a genetic factor contributing to heritability of low circulating plasma renin and CKD in a small group of African-Americans. We were unable to recruit and study any individuals with the p.R33W mutation, who could have mild hyperkalemia, gout, and CKD with aging.

While this is the largest study of patients with ADTKD-*REN*, the small number of participants still limited our ability to assess the effects of fludrocortisone. Moreover, data was limited in teenage males and patients in the mature group. As the study was retrospective and these individuals were asymptomatic, there was no need for clinicians to perform laboratory studies earlier in life. We are interested in adding further families to our registry in order to improve clinical characterization, and we would appreciate information on other families with this disorder (please contact ableyer@wakehealth.edu).

In summary, families with ADTKD-*REN* can be divided into three groups. Patients with mutations in the region encoding the mature peptide present with gout in early adulthood or CKD later

in life. Their course is milder than in patients with mutations in the regions encoding the signal peptide and prosegment. In these latter two groups, kidney function appears to be decreased starting from birth in many patients but remains stable through early adulthood. Anemia, hyperkalemia, and acidosis are frequently present, with acidosis being inadequately treated in a number of patients. Fludrocortisone raises eGFR, lowers serum potassium, and improves serum bicarbonate, but only a few patients received treatment with this medication, limiting our abilities to understand advantages and disadvantages of treatment.

METHODS

This investigation was approved by the institutional review boards of the participating centers and was carried out in accordance with the Declaration of Helsinki.

Identification of cases

Between January 1, 2019 and February 29, 2020, the literature was reviewed for families reported with heterozygous *REN* mutations, and the authors were contacted for additional information regarding affected patients. Academic centers with an interest in ADTKD were contacted and asked to provide clinical and genetic data from families with ADTKD-*REN* that had not been reported (**Supplementary Figure S1**). Investigators were asked to provide the following information for each individual from birth through February 29, 2020: mutation, age and reason for presentation, all hemoglobin values and use of erythropoietin, all serum electrolyte, uric acid, blood urea nitrogen and creatinine values, the age of onset of ESKD, and the use of fludrocortisone, allopurinol, or alkali supplementation. These mutations were not present in the Genome Aggregation Database (36) and segregated with disease in affected families, with the exception of p.S45N, which was found not to segregate with disease in the one family found to have this mutation.

Genetic evaluation

REN mutations were identified using either Sanger sequencing of individual *REN* exons, panel sequencing or whole exome sequencing essentially as described (4, 5).

Calculation of estimated glomerular filtration rate

The estimated glomerular filtration rate (eGFR) was determined using the Pottel equation (37). This equation takes into account age, gender, and serum creatinine values. It was specifically chosen because it has been shown to be accurate in all age groups and allows for a continued comparison of data from childhood into adulthood (37), a critical period of analysis in this cohort.

Statistical analysis

Statistical analysis was carried out using SAS statistical software (Cary, NC), using standard analytical tests such as the T-test, Chi-squared test, multivariate regression, and Cox proportional hazards regression. For comparison of laboratory values (including serum potassium, uric acid, hemoglobin, and bicarbonate), the mean values for each patient were determined and compared with the mean values of other patients. This analysis was chosen to maximize the use of data while also controlling for an increased number of measurements for some individuals.

In *silico* analysis

Properties of the signal sequences were assessed as described (5, 6). Mutations were mapped into the prorenin structure (PDB ID 3VCM). Structural models were visualized using Pymol Viewer (DeLano Scientific Palo Alto, CA, USA).

Transient expression of preprorenin in HEK293 cells

Wild type *REN* cloned into pCR3.1 a eukaryotic expression vector was used and corresponding mutated constructs were prepared by site-directed mutagenesis as in our previous study (5, 6). Transfection,

qualitative and quantitative assays and immunofluorescence analysis of renin were performed as described in (5, 6) and in **Supplementary methods**.

DISCLOSURE STATEMENT

Authors have nothing to disclose.

ACKNOWLEDGEMENTS

We thank all participating patients and families, and the referring physicians. We thank Dr. Heike Göbel (Institute of Pathology, University Hospital of Cologne, Cologne, Germany) and Dr. Helmut Hopfer (Institute of Pathology, University Hospital Basel, Basel, Switzerland) for providing renal sections. This study was supported by grant NV17-29786A from the Ministry of Health of the Czech Republic and by institutional programs of Charles University in Prague (UNCE/MED/007 and PROGRES-Q26/LF1). The National Center for Medical Genomics (LM2018132) kindly provided sequencing and genotyping. AJB was funded by the Slim Health Foundation, the Black-Brogan Foundation, and NIH-NIDDK R21 DK106584. KT was supported by MTA-SE Lendulet Research Grant (LP2015-11/2015). JAS is supported by Kidney Research UK and the Northern Counties Kidney Research Fund. BBB and AW were supported by intramural grants from the Koeln Fortune Program/Faculty of Medicine (grant KF Nr 245/2011, grant KF Nr 172/2013, and grant KF 472/18), University of Cologne, Germany. LR was supported by the Italian Society of Nephrology (SIN) under the “Adotta un progetto di ricerca” program, Telethon-Italy (GGP14263); the Italian Ministry of Health (grant RF-2010-2319394), Soli Deo Gloria.

REFERENCES

1. Devuyst O, Olinger E, Weber S, et al. Autosomal dominant tubulointerstitial kidney disease. *Nat Rev Dis Primers*. 2019;5:60.

2. Hart TC, Gorry MC, Hart PS, et al. Mutations of the UMOD gene are responsible for medullary cystic kidney disease 2 and familial juvenile hyperuricaemic nephropathy. *J Med Genet*. 2002;39:882-892.

3. Kirby A, Gnirke A, Jaffe DB, et al. Mutations causing medullary cystic kidney disease type 1 lie in a large VNTR in MUC1 missed by massively parallel sequencing. *Nat Genet*. 2013;45:288-393.

4. Bolar NA, Golzio C, Zivna M, et al. Heterozygous Loss-of-Function SEC61A1 Mutations Cause Autosomal-Dominant Tubulo-Interstitial and Glomerulocystic Kidney Disease with Anemia. *Am J Hum Genet*. 2016;99:174-187.

5. Zivna M, Hulkova H, Marignon M, et al. Dominant renin gene mutations associated with early-onset hyperuricemia, anemia, and CKD. *Am J Human Genet*. 2009;85:204-213.

6. Bleyer AJ, Zivna M, Hulkova H, et al. Clinical and molecular characterization of a family with a dominant renin gene mutation and response to treatment with fludrocortisone. *Clin Nephrol*. 2010;74:411-422.

7. Beck BB, Trachtman H, Gitman M, et al. Autosomal dominant mutation in the signal peptide of renin in a kindred with anemia, hyperuricemia, and CKD. *Am J Kidney Dis*. 2011;58:821-825.

8. Clissold RL, Clarke HC, Spasic-Boskovic O, et al. Discovery of a novel dominant mutation in the REN gene after forty years of renal disease: a case report. *BMC Nephrol*. 2017;18:234.

9. Petrijan T, Menih M. Discovery of a Novel Mutation in the REN Gene in Patient With Chronic Progressive Kidney Disease of Unknown Etiology Presenting With Acute Spontaneous Carotid Artery Dissection. *J Stroke Cerebrovasc Dis*. 2019;28:104302.

10. Abdelwahed M, Chaabouni Y, Michel-Calemard L, et al. A novel disease-causing mutation in the Renin gene in a Tunisian family with autosomal dominant tubulointerstitial kidney disease. *Int J Biochem Cell Biol*. 2019;117:105625.

11. Schaeffer C, Izzi C, Vettori A, et al. Autosomal Dominant Tubulointerstitial Kidney Disease with Adult Onset due to a Novel Renin Mutation Mapping in the Mature Protein. *Sci Rep*. 2019;9:11601.

12. Gribouval O, Gonzales M, Neuhaus T, et al. Mutations in genes in the renin-angiotensin system are associated with autosomal recessive renal tubular dysgenesis. *Nat Genet*. 2005;37:964-968.

13. Gomez RA, Sequiera-Lopez MLS. Renin cells in homeostasis, regeneration and immune defence mechanisms. *Nat Rev Nephrol*. 2018;14:231-245.

14. Pugliese NR, Masi S, Taddei S. The renin-angiotensin-aldosterone system: a crossroad from arterial hypertension to heart failure. *Heart Fail Rev.* 2020;25:31-42.

15. Sparks MA, Crowley SD, Gurley SB, Mirotsou M, Coffman TM. Classical Renin-Angiotensis system in kidney physiology. *Compr Physiol*. 2014;4:1201-1228.

16. Imai T, Miyazaki H, Hirose S, et al. Cloning and sequence analysis of cDNA for human renin precursor. *Proc Natl Acad Sci USA*. 1983;80:7405-7409.

17. Schweda F, Friis U, Wagner C, et al. Renin release. *Physiology (Bethesda)*. 2007;22:310-319.

18. Sagnella GA. Why is plasma renin activity lower in populations of African origin? *J Hum Hypertens.* 2001;15:17-25.

19. Petersen TN, Brunak S, von Heijne G, Nielsen H. SignalP 4.0: discriminating signal peptides from transmembrane regions. *Nat Methods*. 2011;8:785-786.

20. Jagadeesh KA, Wenger AM, Berger MJ, et al. M-CAP eliminates a majority of variants of uncertain significance in clinical exomes at high sensitivity. *Nat Genet*. 2016;48:1581-1586.

21. Nagahama M, Nakayama K, Hori H, Murakami K. Expression of a deletion mutant of the prosegment of human prorenin in Chinese hamster ovary cells. *FEBS Lett*. 1989;259:202-204.

22. Nakayama K, Nagahama M, Kim WS, et al. Prorenin is sorted into the regulated secretory pathway independent of its processing to renin in mouse pituitary AtT-20 cells. *FEBS Lett*. 1989;257:89-92.

23. Mercure C, Thibault G, Lussier-Cacan S, et al. Molecular analysis of human prorenin prosegment variants in vitro and in vivo. *J Biol Chem*. 1995;270:16355-16359.

24. Guo H, Xiong Y, Witkowski P, et al. Inefficient translocation of preproinsulin contributes to pancreatic beta cell failure and late-onset diabetes. *J Biol Chem*. 2014;289:16290-16302.

25. Liu M, Lara-Lemus R, Shan SO, et al. Impaired cleavage of preproinsulin signal peptide linked to autosomal-dominant diabetes. *Diabetes*. 2012;61:828-837.

26. Arnold A, Horst SA, Gardella TJ, et al. Mutation of the signal peptide-encoding region of the preproparathyroid hormone gene in familial isolated hypoparathyroidism. *J Clin Invest*. 1990;86:1084-1087.

27. Hussain S, Mohd Ali J, Jalaludin MY, Harun F. Permanent neonatal diabetes due to a novel insulin signal peptide mutation. *Pediatr Diabetes*. 2013;14:299-303.

28. Demidyuk IV, Shubin AV, Gasanov EV, Kostrov SV. Propeptides as modulators of functional activity of proteases. *Biomol Concepts*. 2010;1:305-322.

29. Weiss MA. Diabetes mellitus due to the toxic misfolding of proinsulin variants. *FEBS Lett*. 2013;587:1942-1950.

30. Bentley AK, Rees DJ, Rizza C, Brownlee GG. Defective propeptide processing of blood clotting factor IX caused by mutation of arginine to glutamine at position -4. *Cell*. 1986;45:343-348.

31. Saraste J, Marie M. Intermediate compartment (IC): from pre-Golgi vacuoles to a semi-autonomous membrane system. *Histochem Cell Biol*. 2018;150:407-430.

32. Liu M, Sun J, Cui J, et al. INS-gene mutations: from genetics and beta cell biology to clinical disease. *Mol Aspects Med*. 2015;42:3-18.

33. Given BD, Mako ME, Tager HS, et al. Diabetes due to secretion of an abnormal insulin. *N Engl J Med*. 1980;302:129-135.

34. Sakura H, Iwamoto Y, Sakamoto Y, et sal Structurally abnormal insulin in a diabetic patient. Characterization of the mutant insulin A3 (Val----Leu) isolated from the pancreas. *J Clin Invest*. 1986;78:1666-16672.

35. Shoelson S, Fickova M, Haneda M, et al. Identification of a mutant human insulin predicted to contain a serine-for-phenylalanine substitution. *Proc Natl Acad Sci US* . 1983;80:7390-7394.

36. Genome Aggregation Database [Available from: https://gnomad.broadinstitute.org/gene/ENSG00000143839?dataset=gnomad_r3.

37. Pottel H, Hoste L, Dubourg L, et al. An estimated glomerular filtration rate equation for the full age spectrum. *Nephrol Dial Transplant*. 2016;31:798-806.

TABLES

Table 1. Distribution of heterozygous mutations causing ADTKD-*REN* mutations by mutation group and family.

Mutation group	Mutation	Families (n)	Individuals (n)
Signal	p.W10R	1	5
	p.L12P	1	1
	p.L13Q	1	1
	p.delL16	6	28
	p.L16P	3	11
	p.L16R	2	9
	p.W17R	4	9
	p.C20R	3	5
Signal total		21	69
Prosegment	p.T26I	2	19
	p.M39K	1	5
	p.E48K	1	3
Prosegment total		4	27

Mature	p.C325R	1	3
	p.I366N	1	2
	p.L381P	1	5
	p.T391R	1	4
	p.Q85H	1	1
Mature Total		5	15
Total		30	111

Table 2. Characteristics according to mutation group.

	Signal	Prosegment	Mature	*P* value
Individuals	69 (62%)	27(24%)	15(14%)	
Families	21(70%)	4(13%)	5(17%)	
Age at presentation[1] < 10	23(39%)	11(61%)	0	0.003
Age at presentation[1] 10 to < 20	19(32%)	2(11%)	0	0.02
Age at presentation[1] >20	17(29%)	5(28%)	12(100%)	<0.001
Age at presentation (mean±s.d.)[1,2]	19.7±15.7	22.4±20.2	37.0±12.4[2]	
Reason for presentation[1,2]				0.014
Acute kidney injury	5/55 (10%)	0	0	
Anemia, acidosis, kidney	7/55(13%)	0	0	

failure				
Anemia	17/55(31%)	7/14(50%)	0	
Chronic kidney disease	12/55(22%)	2/14(14%)	3/12(25%)	
Gout	14/55(25%)	5/14(36%)	9/12(75%)	
Total	55	14	12	
Anemia as child (%)	39/43(91%)	11/16(69%)	0/7(0%)	<0.001
Gout developed during the course of disease (%)	31/55(56%)	13/20(65%)	9/14(64%)	0.74
Age at first gout attack (mean±s.d.)	29.7±9.9	25.7±8.2	32.9±11.2	0.4
Age at ESKD onset (mean±s.d.)	53.1±10.6	50.8±17.6	63.6±7.6[2]	

[1]Excluding individuals who presented for asymptomatic genetic screening. Six of 61 (10%) in the signal group, 7/21 (33%) in the prosegment group, and 3/15 (20%) patients in the mature group were identified by asymptomatic genetic screening.

[2]$p<0.001$ when compared to the two other groups.

Table 3. Proportional hazards models including all individuals, with the event being age of end-stage kidney disease (ESKD). The univariate model showing anemia in childhood was also the best-fit multivariate model.

Model	Risk	Reference	Hazard ratio	*P* value
Univariate	Mutation affecting mature renin	Mutations affecting signal peptide and prosegment	0.367	0.023
Univariate	Anemia in childhood	No anemia in childhood or unknown	2.82	0.003
Univariate	Male	Female	0.92	0.80

Table 4. Characteristics of presentation according to gender for patients with signal peptide or prosegment mutations.

	Female	Male	*P* value
Individuals	44	52	0.41
Age at presentation[1] < 10	18/35(48.6%)	17/43(39.5)	0.42
Age at presentation[1] 10 to < 20	9/35(25.7%)	12/43(27.9%)	0.85
Age at presentation[1] >20	9/35(25.7)	13/43(30.2%)	0.66
Age at presentation (mean±s.d.)	19.9±19.4	19.3±13.7	0.6
Anemia as child (%)	31/32(96.7%)	19/27(45.8%)	0.005
Gout (%)	15/38(39.5%)	29/37(49.3%)	0.0006
Age at first gout attack (mean±s.d.)	30.3±9.6	27.8±9.7	0.45
Age at ESKD onset (mean±s.d.)	50.1±11.4	55.8±10.5	0.25
Serum potassium (mEq/L) (mean±s.d.)	5.1±0.5	5.1±0.6	0.75
Serum bicarbonate (mEq/L) (mean±s.d.)	21.3±0.4	22.2±2.5	0.38

Serum urate (mg/dL) without urate-lowering therapy (mean±s.d.)	7.7±1.6	9.4±2.7	0.02

[1]Excluding individuals who presented for asymptomatic genetic screening.

Table 5 REN mutations; a summary of *in vitro* characteristics

	Cell lyzate				Culturing medium							Cellular localization
Localization of the mutation	Preprorenin (WB)	Prorenin (WB) IRMA % of wild type renin	Renin (WB) IRMA % of wild type)	Prorenin / Renin ratio	Prorenin (WB)	Renin (WB)	Prorenin IRMA assay % of wild type renin	Renin IRMA assay % of wild type renin	Prorenin / Renin ratio	Prorenin activity % of wild type renin	Renin activity % of wild type renin	Prorenin / Renin ratio	Immunofluorescence using anti-human preprorenin 288-317 antibody detecting preprorenin + prorenin + renin
wild type protein	+	+ 112±19	+ 100±13	1.1	+	-	705±71	100±4	7.5	100±6	100±4	1	Coarsely granular structures in cytoplasm and lysosomes
signal peptide del16L	+	+ 4±3	+ 77±1	0.1	+	-	457±41	61±1	7.5	27±1	21±3	1.3	Less distinct granular structures in cytoplasm and lysosomes
signal peptide missense	+	- 2-3	- 2-6	0	-	-	51-85	7-15	0	3-10	0-7	0	Diffuse cytoplasmic staining
prosegment T26I	+	+ 72	+ 112	0.6	+	-	167±19	130±11	1.3	87	72	1.2	Less distinct granular structures in cytoplasm and lysosomes with diffuse staining localized partly to ERGIC
prosegment M39K	+	+ 67	+ 81	0.8	+	-	7±33	238±24	0.03	64	255	0.25	
prosegment VUS_S45N	+	+ 119±23	+ 64 ±16	1.9	+	-	768±170	66±12	11.6	97±4	88±5	1.1	
mature renin C325R	-	+ 5	+ 7	0	-	-	0	0	0	0.1±0.1	0	0	Intracellular clumps localized to ER
AA variants													
signal peptide P8A	+	+ 132±26	+ 89±16	1.5	+	-	658±29	73±14	9	102±2	109±5	0.9	Similar to wild type
prosegment R33W	+	+ 22±6	+ 30±3	0.7	+	-	67±7	74±22	0.9	37±1	103±5	0.4	More diffuse pattern localized to ERGIC

Gray-shaded values are those significantly different from the wild type.

FIGURE LEGENDS

Figure 1. Age vs. estimated glomerular filtration rate (eGFR) in ADTKD-*REN* patients. A. All estimated glomerular filtration rate (eGFR) measurements for each group are included (signal group green, prosegment group red, mature group black). A best-fit line is included for each group. Patients in the mature group presented later in life and had normal kidney function at earliest measurement. Patients in the signal and prosegment group often presented early in life, and eGFR was significantly decreased from the time of first measurement in most patients. **B.** eGFR values in 13 children with longitudinal follow-up from the signal group. Each child is represented by a different color with a best-fit line, and the *REN* mutation is given in the legend. Despite having low eGFR values at earliest measurement, kidney function remained stable until age 20 in most patients.

Figure 2. End-stage kidney disease (ESKD) survival in ADTKD-*REN* individuals according to *REN* mutation group. This analysis included 111 individuals. An event was defined as starting dialysis or receiving a transplant. Censoring occurred if the individual had not reached ESKD by the end of the study period. Patients in the mature group had a later age of onset of ESKD compared to the signal and prosegment groups (hazards ratio = 0.237, p=0.023).

Figure 3. End-stage kidney disease (ESKD) survival according to presence of anemia in childhood. This analysis included 111 ADTKD-*REN* individuals. An event was defined as starting dialysis or receiving a transplant. Censoring occurred if the individual had not reached ESKD by the end of the study period. A diagnosis of anemia in childhood was associated with a worse prognosis (hazard ration 2.82, p=0.03).

Figure 4. Hemoglobin, hyperkalemia and acidemia in ADTKD-*REN* patients. White circles represent females and black circles represent males. **A.** Hemoglobin values according to age. For females, hemoglobin values were low throughout the period of measurement. For males, hemoglobin values began to rise at age 20. **B**. Serum potassium values according to age. Values remained consistent over time. **C.** Serum potassium according to estimated glomerular filtration rate (eGFR). **D.** Serum bicarbonate values according to age. There were many serum bicarbonate values <24 mEq/l.

Figure 5. ADTKD-*REN* treatment with fludrocortisone. This figure includes 13 young patients in signal (n=11) and prosegment groups (n=2), mutations are listed in the legend. The patient denoted with burgundy markers began fludrocortisone age 11, with an increase in eGFR that was sustained. The patient denoted with red markers started fludrocortisone at age 13.

Figure 6. *In silico* analysis of *REN* variants. (A) Preprorenin, a precursor of prorenin and renin, consists of : i) the signal peptide (SP) essential for targeting and insertion of the synthesized protein into the endoplasmic reticulum membrane, ii) the prosegment that determines the biosynthesis, cellular trafficking and enzymatic activity and iii) the mature enzymatically active renin that is formed upon the proteolytic cleavage of prorenin. Novel pathogenic mutations identified and characterized in this study are shown in red. Previously reported dominant mutations associated with ADTKD are shown in green. The p.S45N is considered nonpathogenic and is shown in blue. Variants of unknown significance identified in African-American variants are shown in yellow. Epitope 288-377 denotes the protein segment recognized by the anti-preprorenin antibody used in this study. The n, h and c regions respectively denote stretches of positively charged amino acids (n-region), hydrophobic amino acids (h-region) essential for targeting and insertion of the signal peptide into ER membrane, and polar amino

acids (c-region), forming a recognition site for the signal peptidase that releases translocated preproprotein from its ER membrane-anchored signal peptide. (**B**) Amino acids conservation across mutated segments of *REN* in higher mammals. Asterisks (*) indicate amino acid residues that are absolutely conserved, a colon (:) indicates residues with strong conservation and a dot (.) indicate residues with weak conservation between species. (**C**) Computational prediction by the SignalP 4.1 server of the impact of missense *REN* mutations located in the signal peptide on the conformation of the signal peptide cleavage site location (C-score) and on the sequence characteristics of the signal peptide (Y-score). SP denotes presence (YES/NO) of the signal peptidase cleavage site within the given sequence. The first 60 N-terminal amino acids of *REN* were used for this calculation. (**D**) Computational prediction by Mendelian Clinically Applicable Pathogenicity Score (M-CAP) of the pathogenicity of missense *REN* mutations located in the propeptide and mature renin.

Figure 7. Structural topology and impact of prosegment and renin mutations. The crystal structure of prorenin (PDB ID 3VCM) was used for modelling. The prorenin segment (amino acid residues 24-66) and the renin core (amino acid residues 67-406) are colored in magenta and green, respectively. The location of mutated residues is shown in the full structural model using red spheres. The effects of each mutation are illustrated in detail at individual images. Mutated residues and their interactions are highlighted as sticks and dashed lines. The mutation p.R33W loses polar contacts with Q241 and D248. Possible compensatory interactions between the proximal two beta-sheets are highlighted as three dashed lines. These changes decrease affinity between prorenin and renin. The mutation p.M39K causes steric clashes and charge repulsion with K100, resulting in decreased affinity between prorenin and renin. The nonpathogenic mutation p.S45N changes the interaction network, with S45 interacting with S41, while N45 interacts with L137 and D139. These changes increase affinity due to a changed interaction network. The mutation p.C325R disrupts a disulfide bridge (highlighted as sticks), and incorporation of

the arginine residue causes steric clashes (shown as red areas). The mutation p.I366Nresults in the loss of hydrophobic contacts (shown by red spheres) in the renin core.

Figure 8. Transient expression and functional characterization of REN variants in Human Embryonic Kidney 293 cells. The wild type renin (WT); signal peptide, prosegment and mature renin mutations; African-American (AA_*REN*) variants and empty vector were analyzed. (**A, B**) Western blot analysis of (**A**) cell lysates and (**B**) culture media. Molecular weights of immuno-reactive proteins present in the WT lysates correspond with expected molecular weights of prorenin (47 kDa), preprorenin (45 kDa) and renin (43 kDa). (**C, D**) Immunoradiometric assay (IRMA) of prorenin and renin amounts in **(C**) cell lysates and (**D**) culture media employing a radio-labeled antibody that specifically recognizes active site of renin. The concentration of prorenin was calculated as the difference between the renin concentration measured before and after trypsin treatment, which activates renin by proteolytic cleavage of the prosegment from prorenin. Amounts of mutated renin (grey bars) and prorenin (black bars) were normalized to the amount of wild type renin. The values represent means ± SD. Measurements were performed in three independent clones for each of the constructs. The individual measurements were carried out in triplicate. The statistical significance of the differences between the WT and renin variants protein amounts was tested by t test. *p < 0.05; **p > 0.01; ***p > 0.001; *n.d.* not done. (**E, F**) Enzymatic activity of (**E**) mature renin secreted into culture media and (**F**) prorenin secreted into culture media. The values were normalized to the WT (100%) and represent means ± SD of relative fluorescent unit (RFU) generated by renin mediated cleavage of the 5-FAM and QXL520 conjugated renin substrate. Measurements were performed in three independent clones for each of the constructs. The individual measurements were carried out in triplicate. The statistical significance of the differences between activity of the wild type renin (WT) and renin variants was tested by t test. *p < 0.05; **p > 0.01; ***p > 0.001; *n.d.* not done.

Figure 9.Transient expression and intracellular localization of transiently expressed mutated preprorenin, prorenin and renin in Human Embryonic Kidney 293 cells.

Preprorenin, prorenin and renin were detected using an antibody recognizing the epitope 288-317 of preprorenin and (**9A**) co-localized with a marker of endoplasmic reticulum intermediate compartment (ERGIC53); wild type protein was present in coarsely granular structures that were localized exclusively in the cytoplasm. Proteins with signal peptide mutations demonstrated either a very similar granular pattern (p.L16del) or intense diffuse cytoplasmic staining; (for detailed renin staining see Supplementary Figure S2). Proteins with prosegment mutations demonstrated a less distinct and more diffuse pattern that was localized mainly to ERGIC. The AA_*REN* variant p.P8A had similar staining pattern to the wild type. The AA_*REN* variant p.R33W demonstrated a less distinct and more diffuse pattern that was localized mainly to the ERGIC. Co-staining of renin with **(B**) protein disulphide isomerase (PDI), a marker of endoplasmic reticulum (ER) demonstrating localization of mature renin mutations in the ER. The degree of renin colocalization with selected markers is demonstrated by the fluorescent signal overlap coefficient values that ranging from 0-1. The resulting overlap coefficient values are presented as the pseudo color which scale is shown in corresponding lookup table.

Figure 10. Pathophysiology of *ADTKD-REN*. (**A**) Wild type preprorenin is cotranslationally translocated into the ER. The signal sequence is cleaved during translocation, and nascent prorenin is glycosylated. Prorenin then transits through the ER-Golgi Intermediate Compartment (ERGIC), which monitors proper protein folding and detects aberrant protein forms. In the Golgi apparatus prorenin is both sorted to clear vesicles and constitutively secreted to proto-granules, where it is proteolytically processed to renin, which is later subjected to regulated secretion. (**B**) Mutations in the signal peptide prevent translocation across the ER membrane, and the preprorenin is aberrantly located in the cytoplasm. This

results in clinical renin deficiency and ER stress in renin producing cells. Mutations in the mature renin lead to retention of mutated protein in ER. This initiates ER stress similar to that seen in *UMOD* mutations and uromodulin retention in ADTKD-*UMOD*. Mutations in the prosegment introduce structural changes affecting protein biosynthesis, folding and travel along the secretory pathway causing clinical renin deficiency and potentially also cellular toxicity leading to chronic kidney disease.

SUPPLEMENTARY MATERIALS

Supplementary Figures

Supplementary Methods

Supplementary References

Figure 1

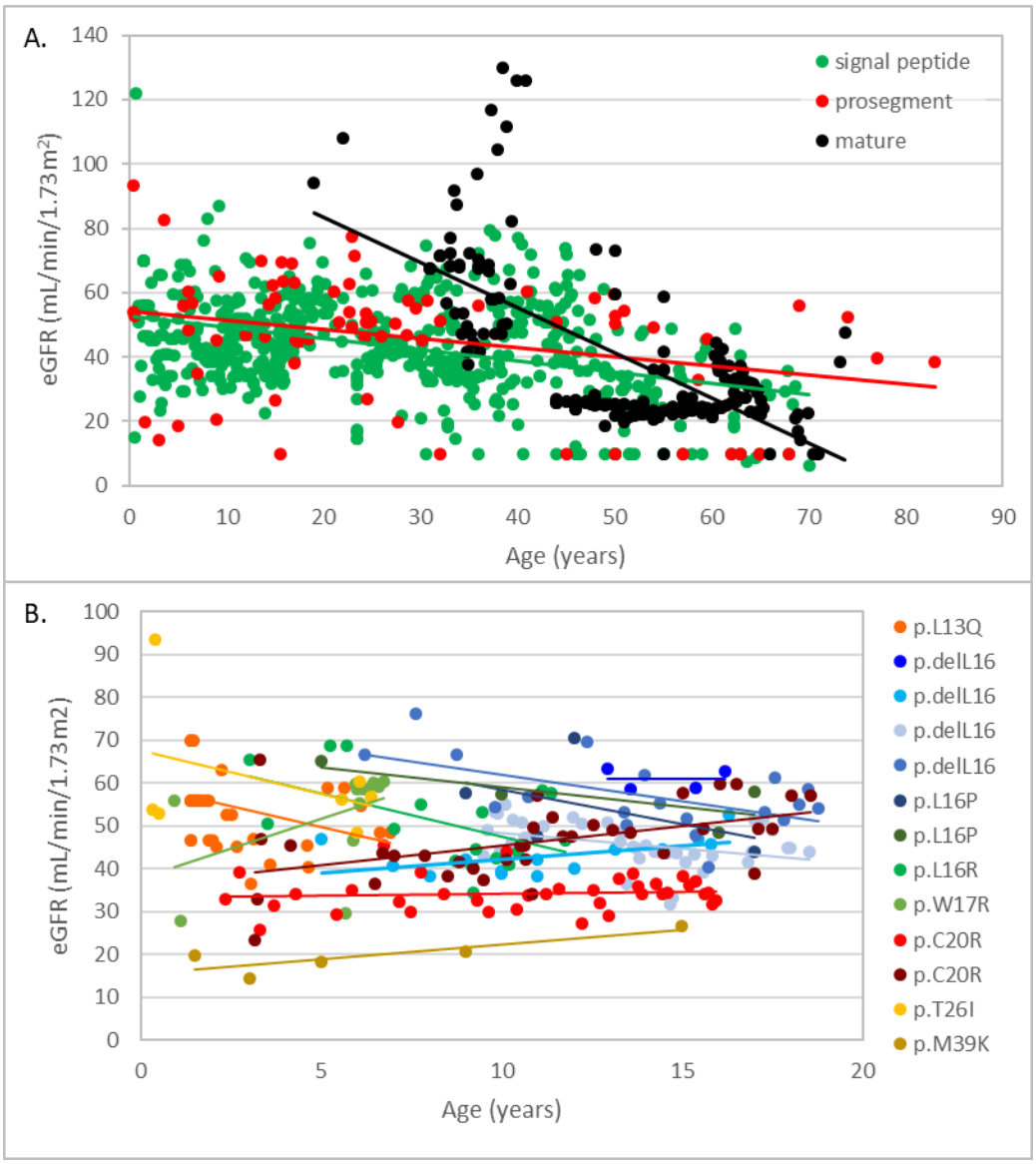
A.
eGFR (mL/min/1.73 m²)
Age (years)
signal peptide
prosegment
mature
B.
eGFR (mL/min/1.73m2)
Age (years)
p.L13Q
p.delL16
p.delL16
p.delL16
p.delL16
p.L16P
p.L16P
p.L16R
p.W17R
p.C20R
p.C20R
p.T26I
p.M39K

Figure 2

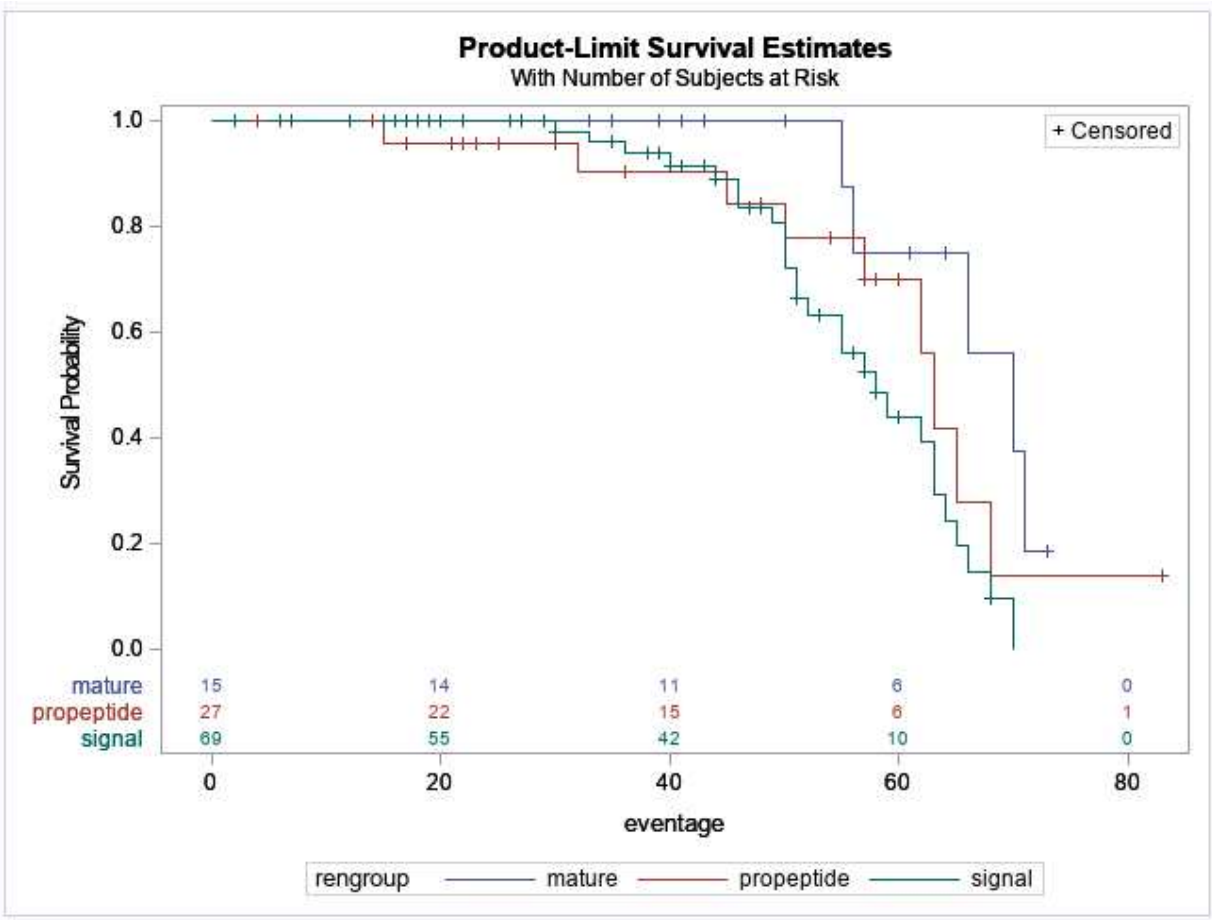
Product-Limit Survival Estimates
With Number of Subjects at Risk
+ Censored
Survival Probability
1.0
0.8
0.6
0.4
0.2
0.0
mature 15 14 11 6 0
propeptide 27 22 15 6 1
signal 69 55 42 10 0
0
20
40
60
80
eventage
rengroup mature propeptide signal

Figure 3

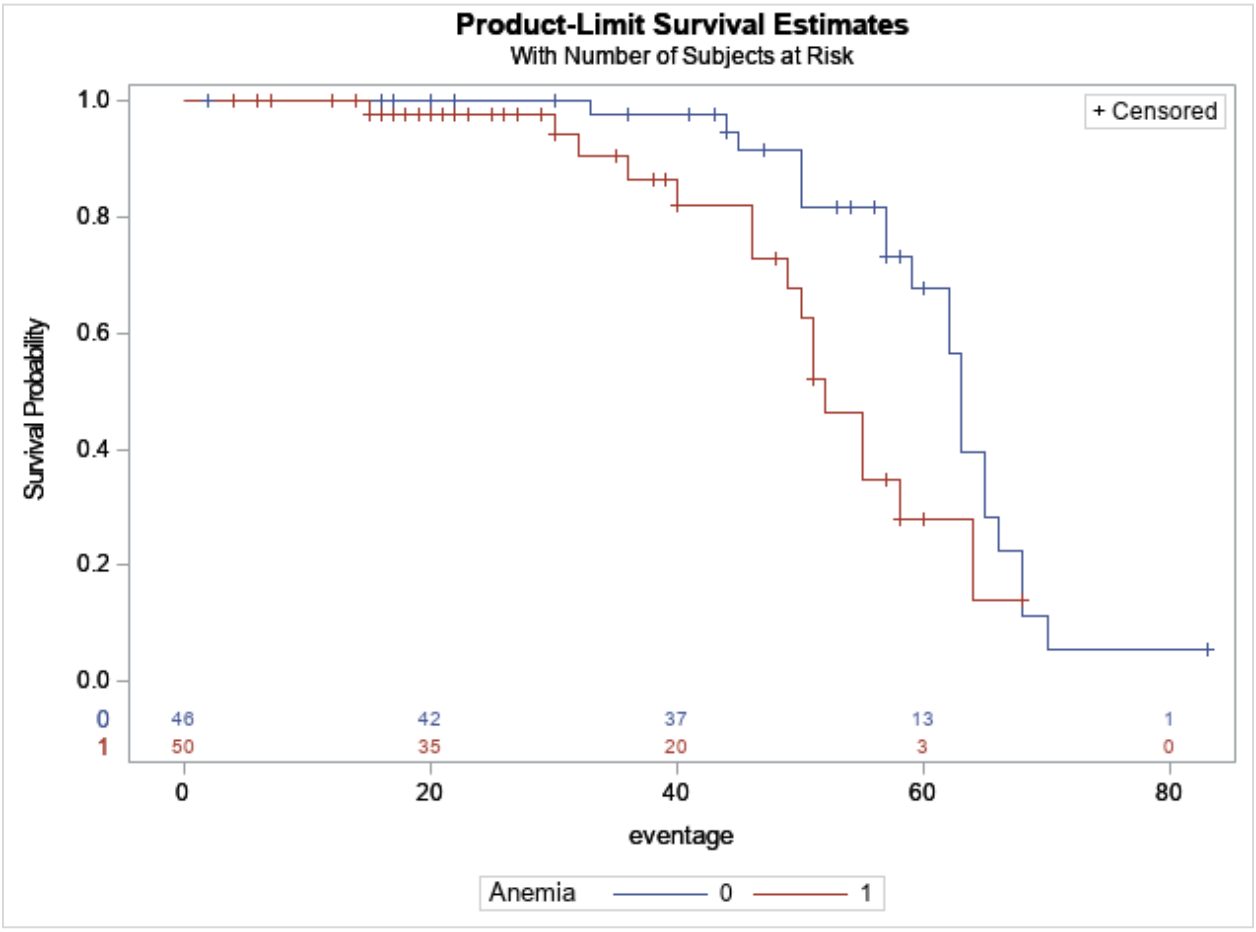
Product-Limit Survival Estimates
With Number of Subjects at Risk
+ Censored
Survival Probability
1.0
0.8
0.6
0.4
0.2
0.0
0 46 42 37 13 1
1 50 35 20 3 0
0
20
40
60
80
eventage
Anemia 0 1

Figure 4

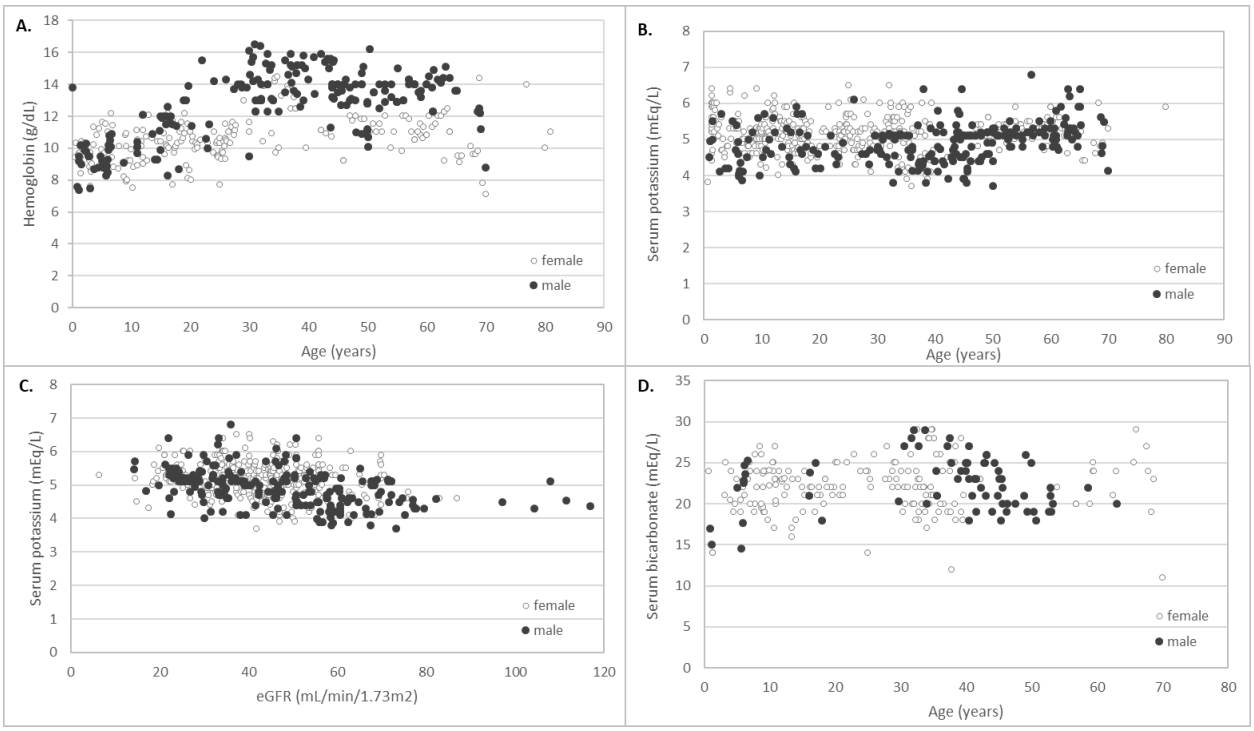
A.
Hemoglobin (g/dL)
Age (years)
female
male
B.
Serum potassium (mEq/L)
Age (years)
female
male
C.
Serum potassium (mEq/L)
eGFR (mL/min/1.73m2)
female
male
D.
Serum bicarbonate (mEq/L)
Age (years)
female
male

Figure 5

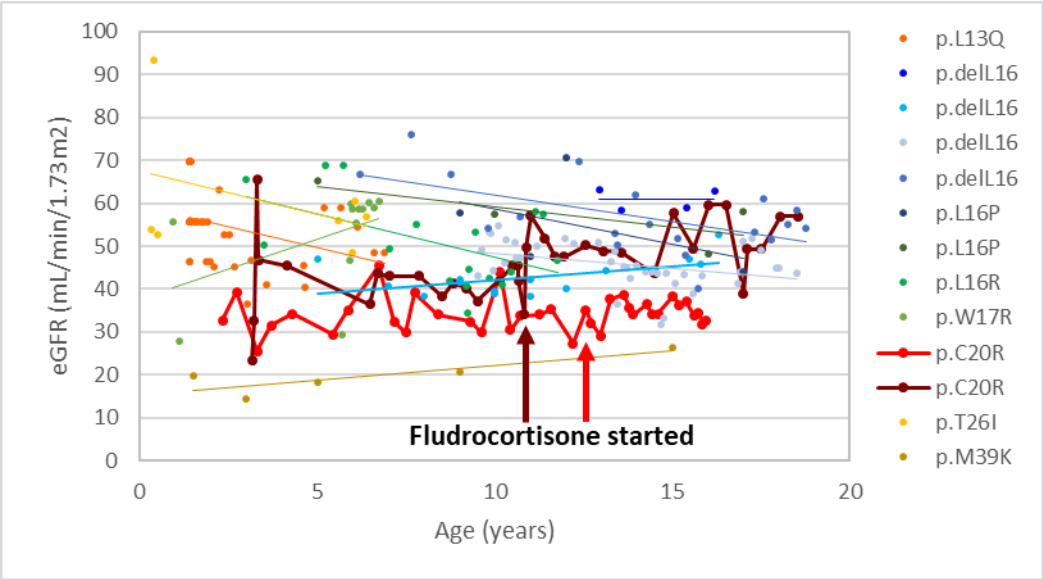
100
90
80
70
60
50
40
30
20
10
0
eGFR (mL/min/1.73m2)
0
5
10
15
20
Age (years)
Fludrocortisone started
p.L13Q
p.delL16
p.delL16
p.delL16
p.delL16
p.L16P
p.L16P
p.L16R
p.W17R
p.C20R
p.C20R
p.T26I
p.M39K

Figure 6

A)

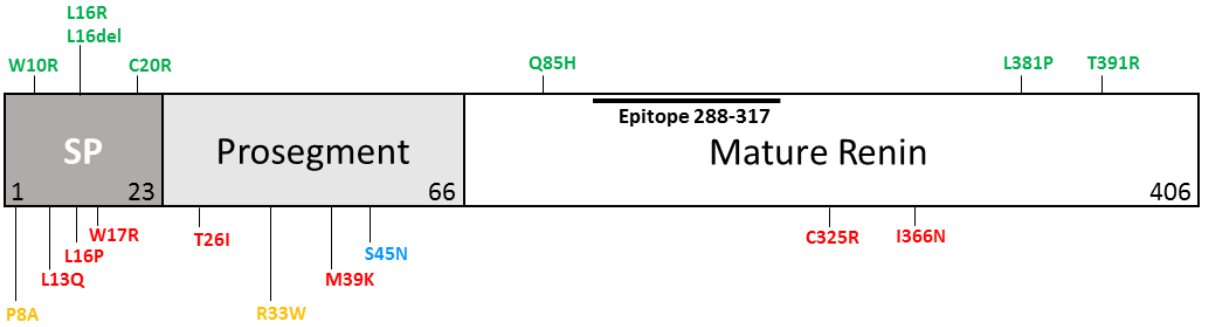

B)

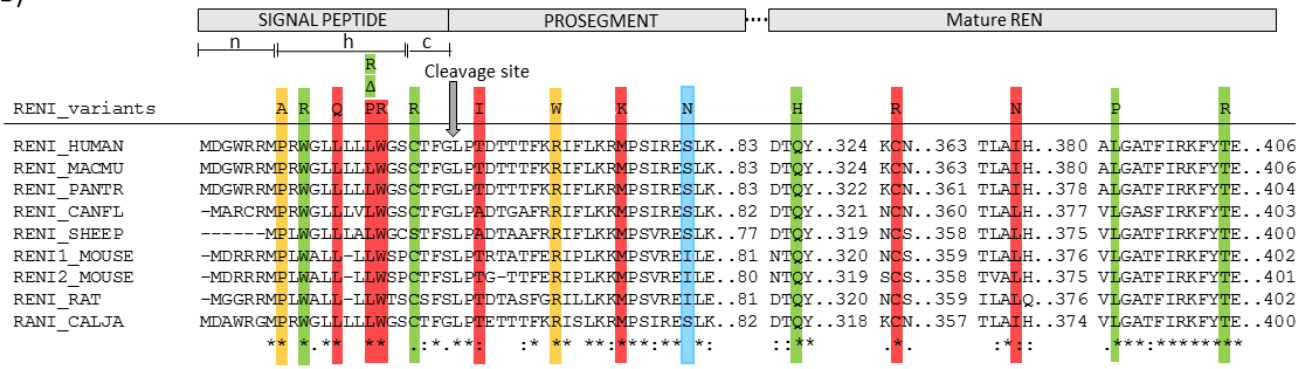

C)

%	Rwt	P8A	W10R	L13Q	delL16	L16R	L16P	W17R	C20R
C-score	100	106	74	57	83	64	56	72	148
Y-score	100	105	82	68	86	73	68	82	142
SP	YES	YES	YES	NO	YES	NO	NO	YES	YES
Type		AA *REN*	reported REF	new	reported REF	reported REF	new	new	reported REF

D)

T26I; c.77C>T	M39K; c.116T>A	S45N; c.134G>A	C325R; c.973T>C	I366N; c.1097T>C	R33W; c.97C>T
0.012 Likely Benign	0.019 Likely Benign	0.007 Likely Benign	0.334 Possibly Pathogenic	0.043 Possibly Pathogenic	0.135 Possibly Pathogenic

Figure 7

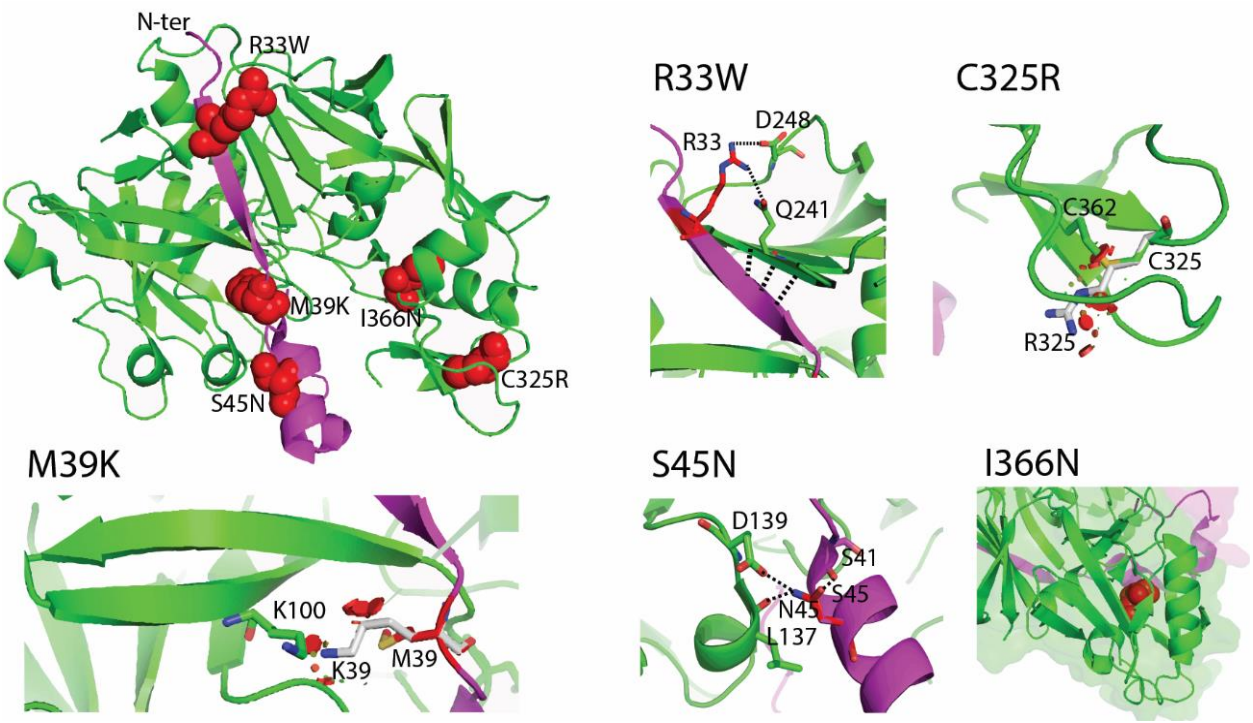
N-ter
R33W
M39K
I366N
S45N
C325R
R33W
D248
R33
Q241
C325R
C362
C325
R325
M39K
K100
M39
K39
S45N
D139
S41
S45
N45
L137
I366N

Figure 8

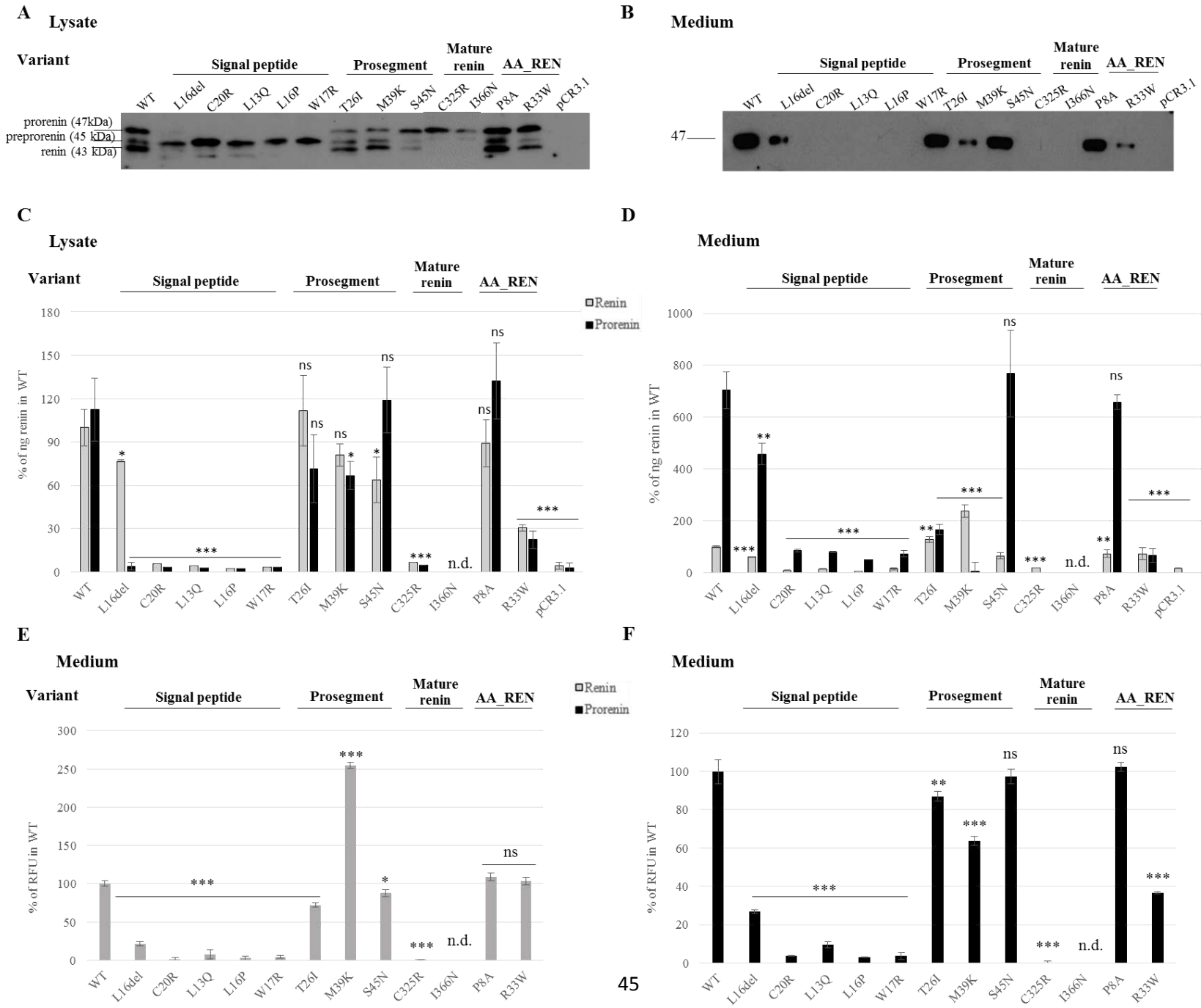
A
Lysate
Variant
Signal peptide
Prosegment
Mature renin
AA_REN
WT
L16del
C20R
L13Q
L16P
W17R
T26I
M39K
S45N
C325R
I366N
P8A
R33W
pCR3.1
prorenin (47kDa)
preprorenin (45 kDa)
renin (43 kDa)
B
Medium
47
C
Lysate
% of ng renin in WT
Renin
Prorenin
n.d.
D
Medium
E
Medium
% of RFU in WT
F
Medium

Figure 9A

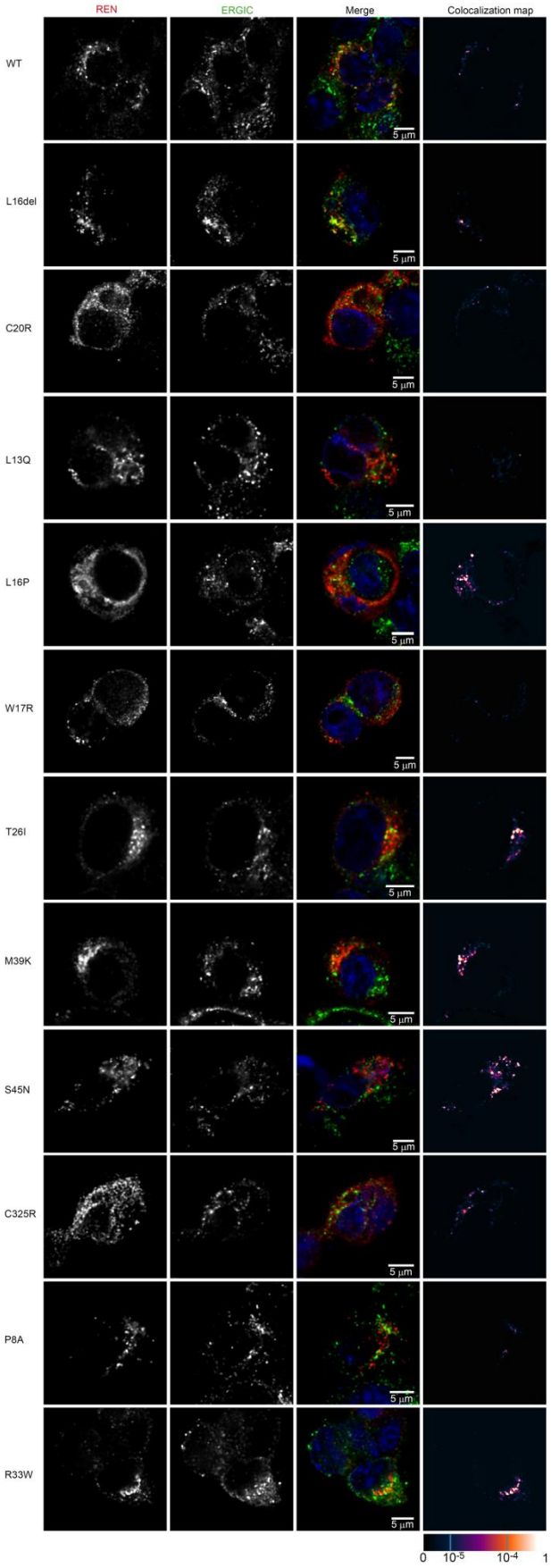
REN
ERGIC
Merge
Colocalization map
WT
L16del
C20R
L13Q
L16P
W17R
T26I
M39K
S45N
C325R
P8A
R33W
5 µm
0
10-5
10-4
1

Figure 9B

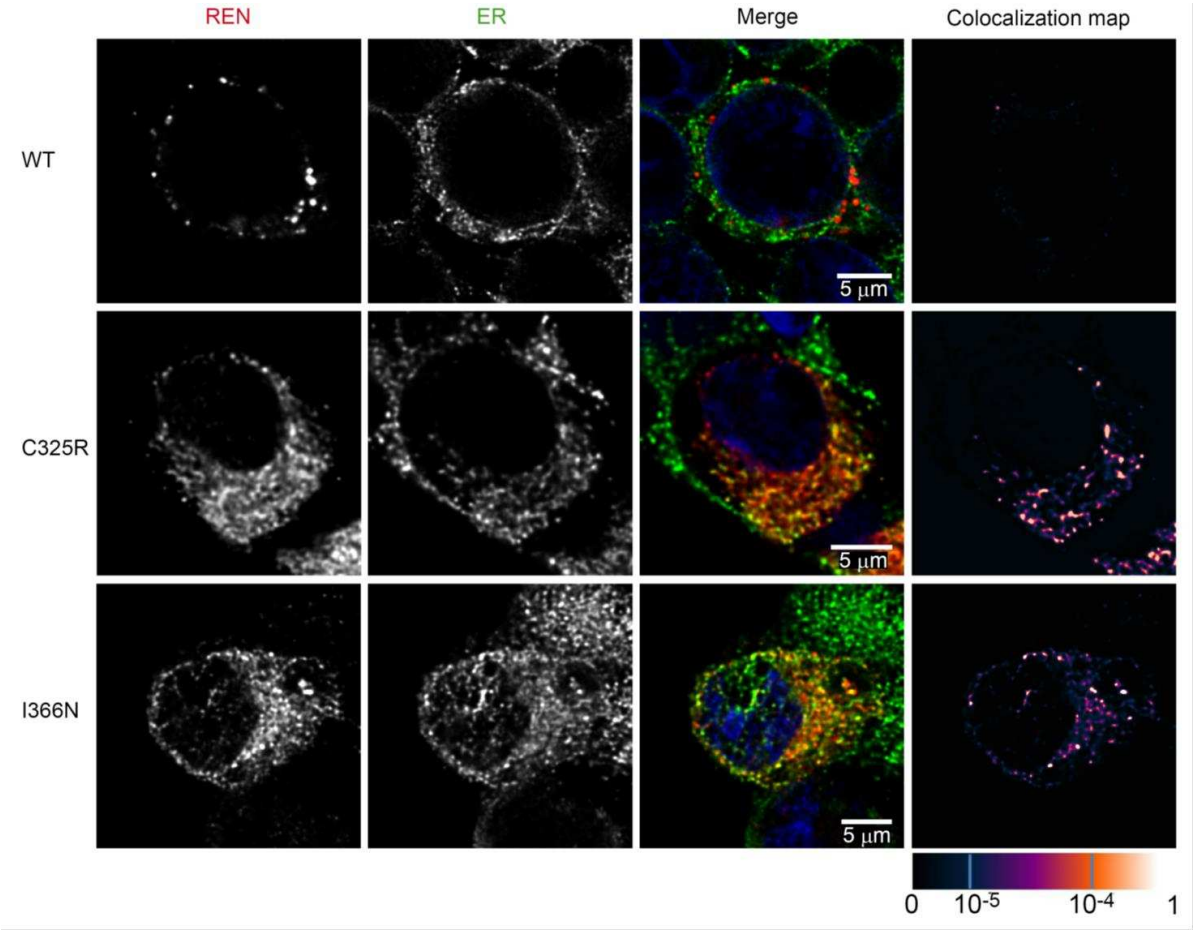
REN
ER
Merge
Colocalization map
WT
C325R
I366N
5 µm
5 µm
5 µm
0
10-5
10-4
1

SUPPLEMENTARY MATERIAL: Distinct subtypes of ADTKD-*REN* in an international cohort study

Figure 10

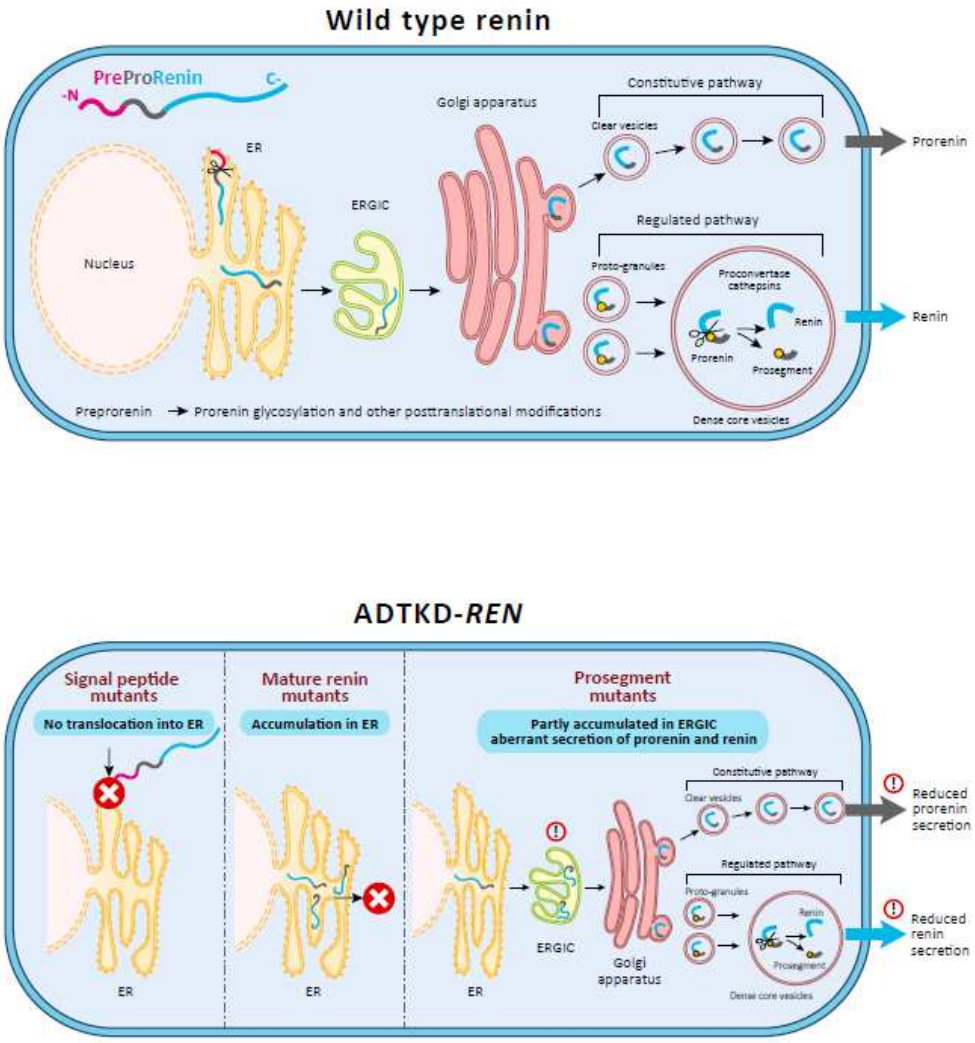

SUPPLEMENTARY MATERIAL

This material provides additional information for the article:

An International Cohort Study of Autosomal Dominant Kidney Disease due to *REN* Mutations Identifies Distinct Subtypes

Authors:

Martina Živná, PhD[1], Kendrah Kidd, MS[1, 2], Mohamad Zaidan, MD, PhD[3], Petr Vyleťal, PhD[1], Veronika Barešová, PhD[1], Kateřina Hodaňová, PhD[1], Jana Sovová[1], Hana Hartmannová, PhD[1], Miroslav Votruba[1], Helena Trešlová[1], Ivana Jedličková [1], Jakub Sikora [1], Helena Hůlková [1], Victoria Robins[2], Aleš Hnízda[4], Jan Živný, PhD[5], Gregory Papagregoriou, PhD[6], Laurent Mesnard, MD[8], Bodo B. Beck [8,9], Andrea Wenzel, PhD[8,9], Kálmán Tory, MD, PhD[10,11], Karsten Häeffner, MD[12], Matthias T.F. Wolf, MD[13], Michael E. Bleyer, BS[2], John A. Sayer, MD PhD[14-16], Albert C. M. Ong, DM[17], Lídia Balogh, MD, PhD[11], Anna Jakubowska, MD[18], Agnieszka Łaszkiewicz, PhD[19], Rhian Clissold, MB ChB, MD[20], Charles Shaw-Smith, MD[20], Raj Munshi, MD[21,22], Robert M. Haws, MD[23], Claudia Izzi, MD[24], Irene Capelli, MD[25], Marisa Santostefano, MD[26], Claudio Graziano, MD[27], Francesco Scolari, MD, PhD[24], Amy Sussman, MD[28], Howard Trachtman, MD[29], Stephane Decramer, MD, PhD[30,31], Marie Matignon, MD[32,33], Philippe Grimbert, MD[32-34], Lawrence R. Shoemaker, MD[35], , Christoforos Stavrou, MD[36], Mayssa Abdelwahed, PhD[37], Neila Belghith, MD[37,38], Matthew Sinclair, MD[39,40], Kathleen Claes, MD, PhD[41,42], Tal Kopel, MD[43], Sharon Moe, MD[44], Constantinos Deltas, PharmR, PhD[6], Bertrand Knebelmann, MD, PhD[45-47], Luca Rampoldi, PhD[48], Stanislav Kmoch, PhD[1, 2], Anthony J. Bleyer, MD, MS[1,2]

Corresponding Author

Anthony J. Bleyer, MD, MS; Wake Forest School of Medicine; Section on Nephrology; Winston-Salem, NC, USA 27157; Fax: 336-716-4318; Phone: 336-716-4650; e-mail: ableyer@wakehealth.edu

SUPPLEMENTARY MATERIAL: Distinct subtypes of ADTKD-*REN* in an international cohort study

Table of Contents

Supplementary Figures

Supplementary Methods

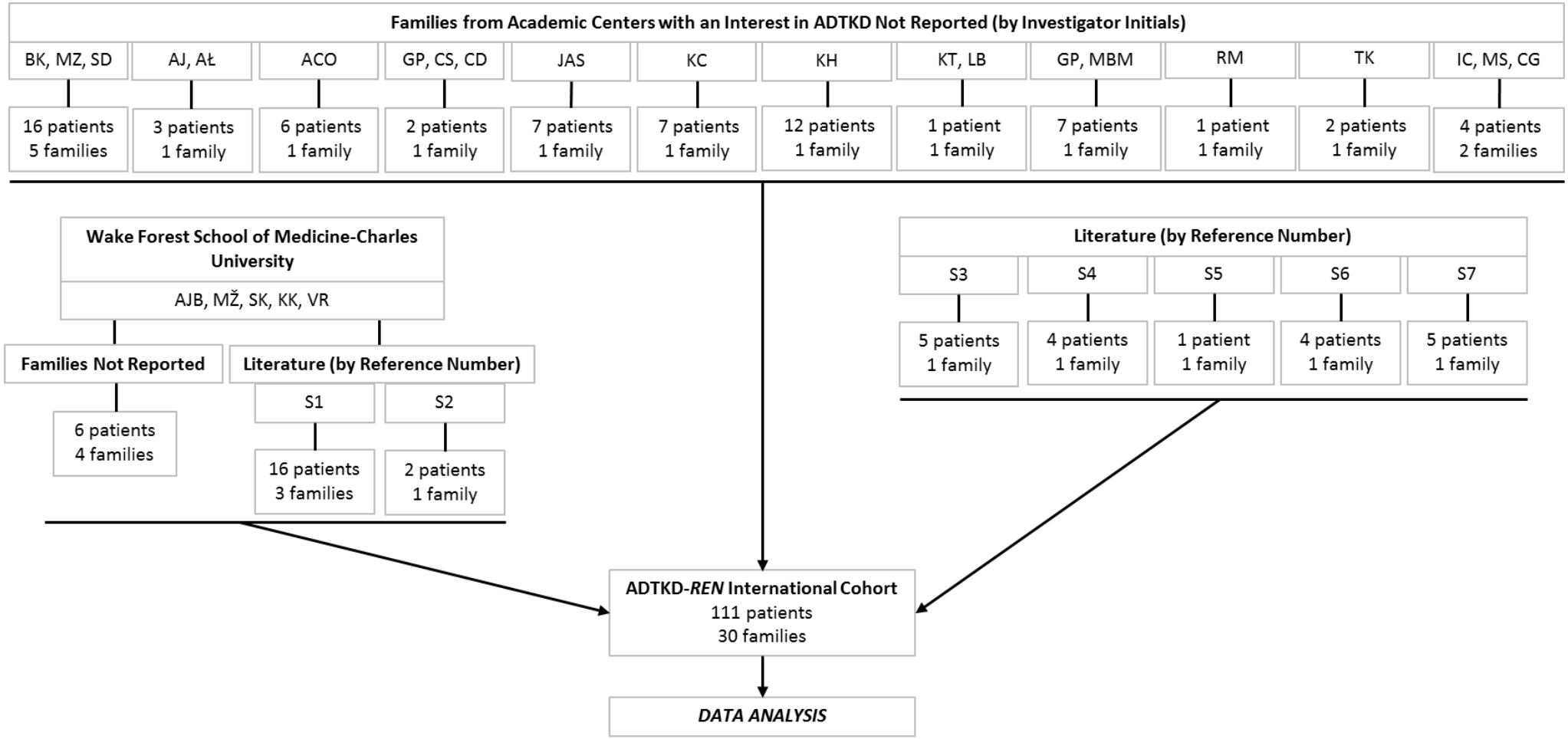

Figure S1. Flow diagram of the ADTKD-*REN* International Cohort. Twelve academic centers with an interest in ADTKD contributed 68 patients from 14 families previously not reported. Wake Forest School of Medicine-Charles University contributed six patients from four families previously not reported and 18 patients from four families published (S1-S2). Literature review yielded five papers describing 19 patients from five families (S3-S7).

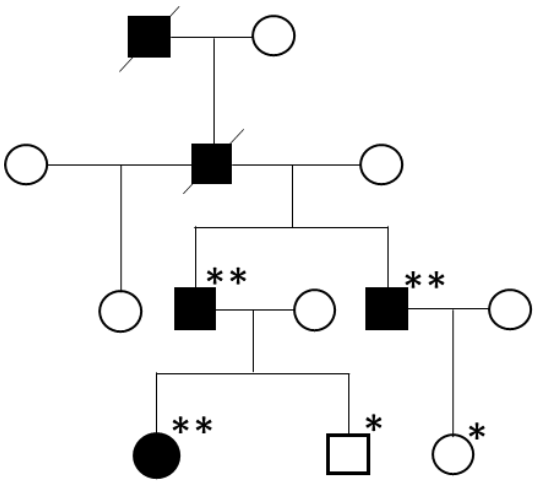

Family A

p.L16del

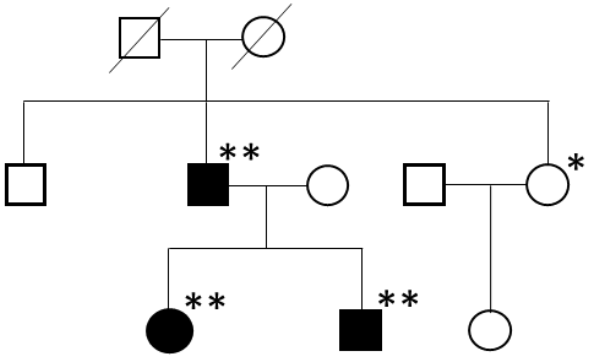

Family B

p.C322R

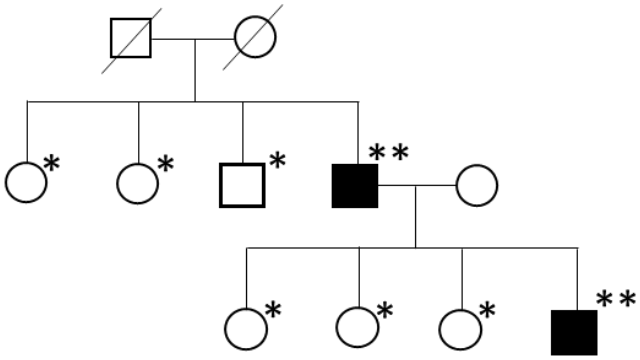

Family C

p.I366N

Figure S2. Representative family trees from three families with dominant *REN* mutations. Clear symbols represent clinically unaffected and filled symbols represent clinically affected. Individuals with 1 asterisk (*) underwent genetic testing and were negative. Individuals with 2 asterisks (**) underwent genetic testing and were positive for a pathogenic *REN* mutation, mutation is given below the family tree. Family trees are also found in references S1-S7.

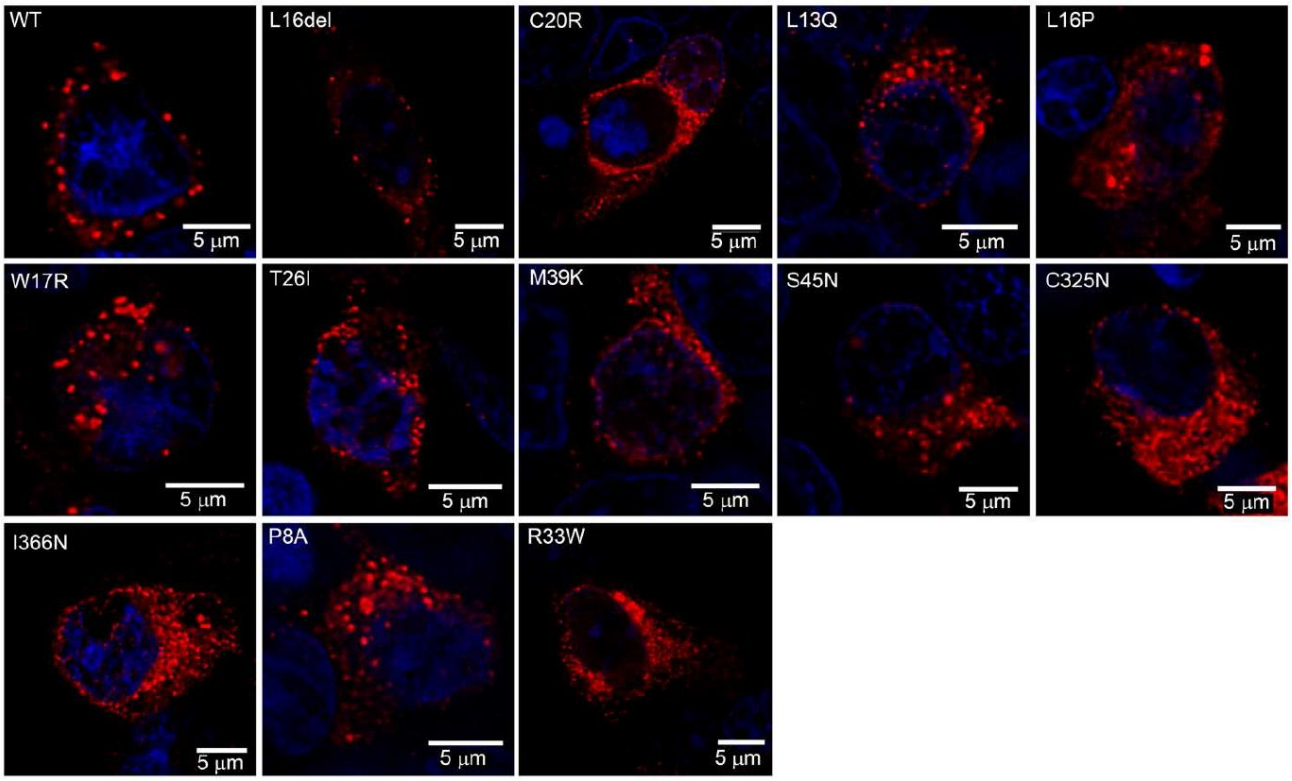

Figure S3. Intracellular localization of transiently expressed mutated preprorenin, prorenin and renin in Human Embryonic Kidney 293 cells. Immunofluorescence detection with an antibody recognizing the epitope 288-317 of preprorenin demonstrates that the wild type protein is present in coarsely granular structures that are localized exclusively in the cytoplasm. Proteins with the mutations in the signal peptide demonstrate either a very similar granular pattern (pL16del) or intense diffuse cytoplasmic staining. Proteins with mutations in the prosegment and renin demonstrate a less distinct and more diffuse pattern.

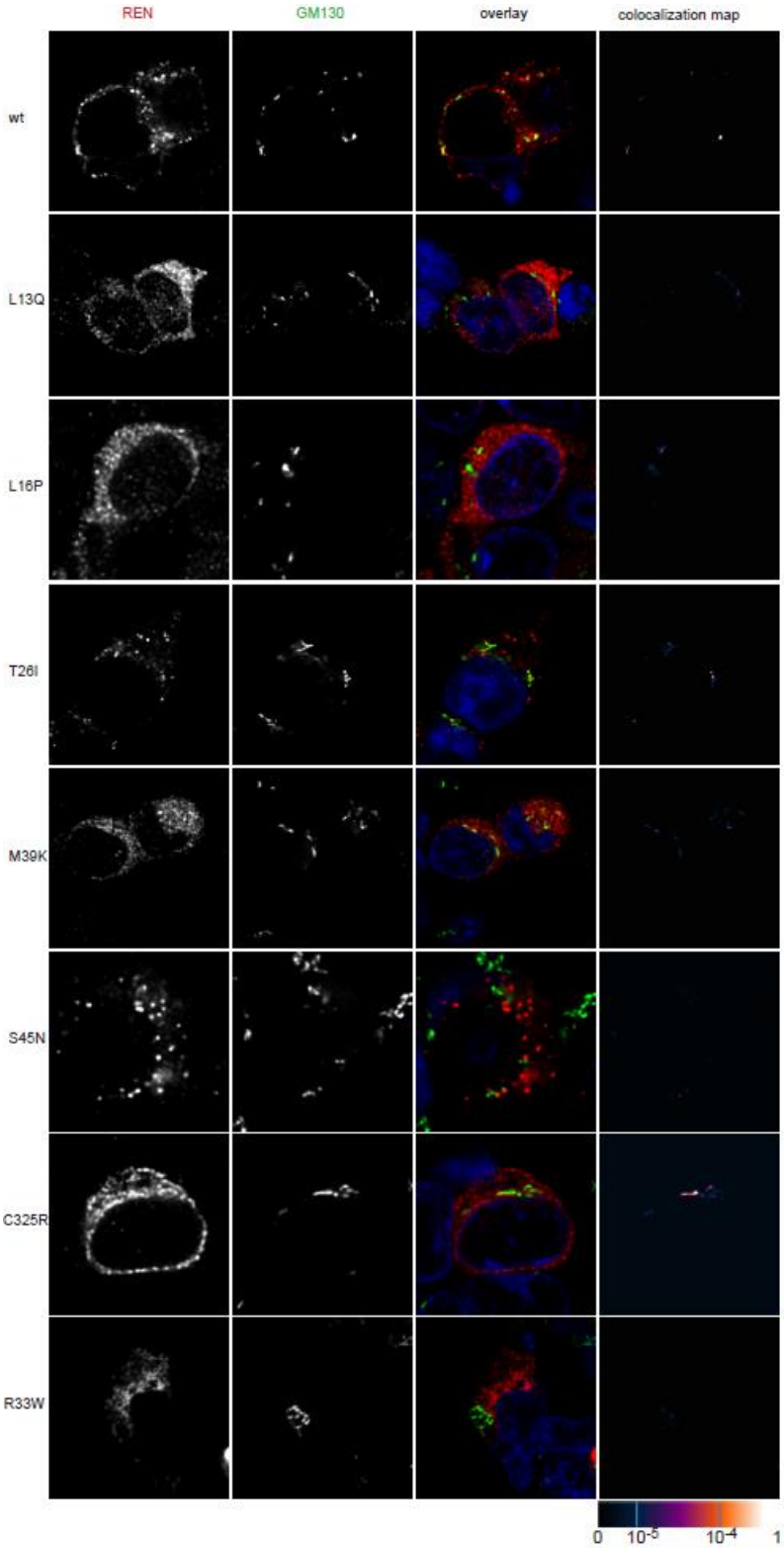
REN
GM130
overlay
colocalization map
wt
L13Q
L16P
T26I
M39K
S45N
C325R
R33W
0
10-5
10-4
1

Figure S4.

Figure S4. Localization of transiently expressed mutated preprorenin, prorenin and renin in Golgi apparatus of Human Embryonic Kidney 293 cells. Immunofluorescent costaining of renin (REN) with an antibody recognizing the epitope 288-317 of preprorenin and Golgi apparatus with mouse anti-GM130 (GM130) showing limited localization of wild type and mutant proteins in Golgi. The degree of renin colocalization with selected marker is demonstrated by the fluorescent signal overlap coefficient values that ranging from 0-1. The resulting overlap coefficient values are presented as the pseudo color which scale is shown in corresponding lookup table.

SUPPLEMENTARY MATERIAL: Distinct subtypes of ADTKD-*REN* in an international cohort study

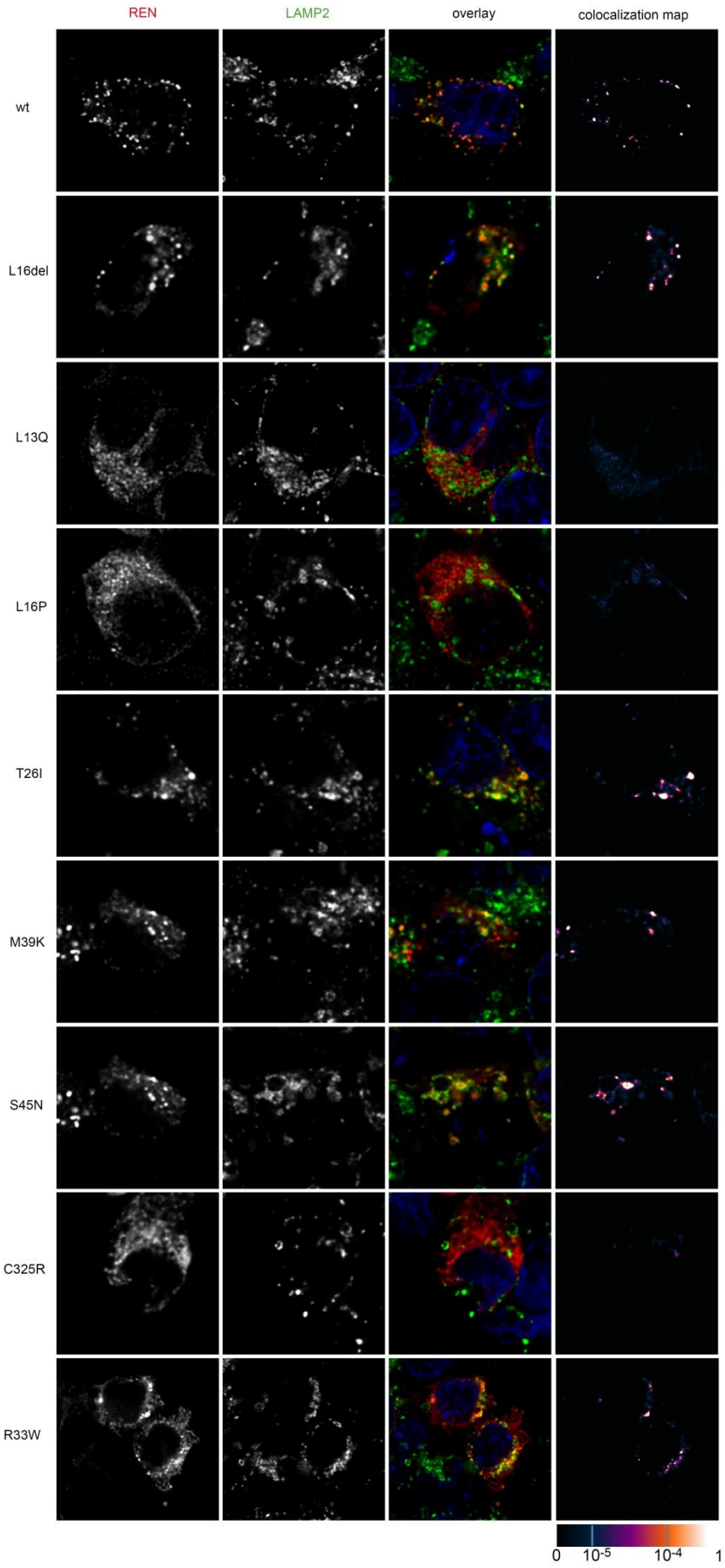

Figure S5.

Figure S5. Localization of transiently expressed mutated preprorenin, prorenin and renin in lysosomes of Human Embryonic Kidney 293 cells. Immunofluorescent costaining of renin (REN) with an antibody recognizing the epitope 288-317 of preprorenin and lysosome with Mouse anti-LAMP2 showing localization of the wild type protein, the protein with signal peptide mutation L16del and proteins with prosegment mutations (T26I, M39K and S45N) in lysosomes. Proteins with other signal peptide mutations (L13Q and L16P) and protein with mutations in the mature renin (C325R) did not localize to lysosomes. The degree of renin colocalization with selected marker is demonstrated by the fluorescent signal overlap coefficient values that ranging from 0-1. The resulting overlap coefficient values are presented as the pseudo color which scale is shown in corresponding lookup table.

Variant	Location	Pearson´s coeficient	Avg	SmOdch
WT		0,18 - 0,22	0.2	0.02
L16del	SP	0,18 - 0,29	0.235	0.055
C20R	SP	0,24 - 0,37	0.305	0.065
L13Q	SP	0,27 - 0,36	0.29	0.02
L16P	SR	0,52 - 0,55	0.535	0.015
W17R	SP	0,25 - 0,31	0.28	0.03
T26I	Prosegment	0,59 - 0,72	0.675	0.085
M39K	Prosegment	0,68 - 0,76	0.72	0.04
S45N	Prosegment	0,69 - 0,84	0.765	0.075
C325R	Mature REN	0,29 - 0,36	0.325	0.035
P8A	AA_REN (SP)	0,12 - 0,32	0.22	0.1
R33W	AA_REN (Pros)	0,59 - 0,66	0.625	0.035

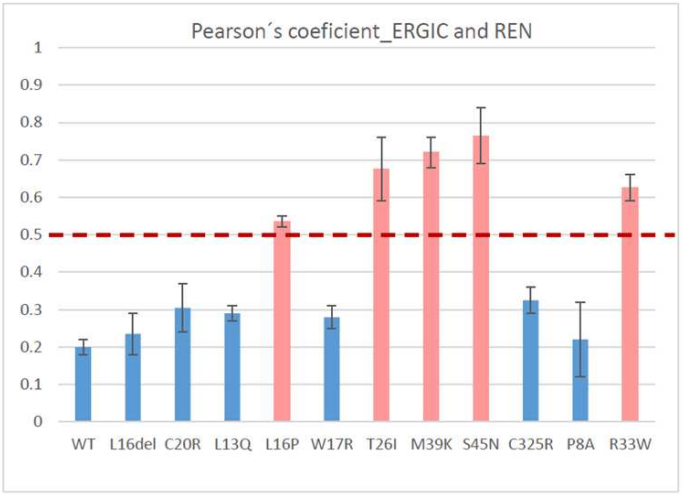

Figure S6. Colocalization of transiently expressed mutated preprorenin, prorenin and renin in ERGIC of Human Embryonic Kidney 293 cells. The Pearson's correlation coefficients of the degree of colocalization of wild type and mutated renin and ERGIC were calculated for 10 transfected cells in the Huygens Professional Software; (y-axis). +1 represents perfect correlation, 0.5 random colocalization and 0 no correlation. Representative immunofluorescence staining is shown in Figure 9.

SUPPLEMENTARY MATERIAL: Distinct subtypes of ADTKD-*REN* in an international cohort study

Supplementary Methods

Transient expression of preprorenin in HEK293 cells

8 x 10^5 HEK 293 cells were seeded on a 6-well plate and grown for 24 hours in DMEM with 10% FCS and 1 mM HEPES (pH 7.31) containing DMEM/F12 media (Gibco) supplemented with 10% fetal calf serum (Gibco) and penicillin / streptomycin at 100 U/ml and 100 µg/ml, respectively, at 37 °C in a 5% CO_2 atmosphere (Sigma). After 24 hours, cells were transfected with Lipofectamine TM2000 with 4µg of appropriate cDNA constructs and grown either in serum-free medium without phenol red (for western blot and enzymatic activity analysis) or fully supplemented medium with phenol red (for IRMA analysis). At 24 hours after transfection, 1 mL media from each type was collected. Cells were mechanically harvested either by PBS1x for quantitative analysis of synthesized renin and prorenin (IRMA method) or lysed by lysis buffer with Protease Inhibitor Cocktail followed by qualitative study (western blot). For IRMA analysis, the amount of renin and prorenin were normalized to total protein concentration in lysates. Total protein concentration was determined using Bradford solution according to the manufacturer protocol (BioRad). Absorbance was measured by the Infinite 200 Pro reader (Tecan, Austria, GmbH) at 595 nm.

Western blot analysis

Cells cultured in FBS and phenol red-free medium were harvested to PBS and pelleted at 800g/7 min/RT. Pellets were resuspended in SDS-PAGE sample buffer (50 mM Tris HCl, 50 mM DTT, 2% SDS, pH 6,8) with Protease Inhibitor Cocktail (Sigma, Prague, Czech Republic) added in a 100:1 ratio and incubated on ice for 3 hours. Lysates were sonicated 3 times for 10 sec with an Ultrasonic Homogenizer 4710 (Cole-Palmer Instruments, Vernon Hills, IL, USA) equipped with cup horn filled with ice cold water, denatured at 100°C/5 min, cooled on ice and stored at -20°C. The protein concentration in lysates was measured by

Direct Detect® Infrared Spectrometer (Merck Millipore, Billarica, MA, USA), according to manufacturer's instructions.

For the secreted renin analysis, FBS and phenol red-free cell culture media were aspirated, mixed with a Protease inhibitor cocktail in 100:1 ratio and successively cleared at 800g/7 min and 15000g/5 min at RT. Supernatants were concentrated on Amicon® Ultra – 0.5mL Centrifugal Filters 10K (Merck Millipore, Tullagreen, Ireland) to minimal volume (about 20 µl) according to manufacturer's instructions. Concentrated media were stored at -20°C.

Volumes of lysates and media equivalent to 15 µg of proteins and 250000 cells, respectively, were mixed with 6X SDS-PAGE sample buffer (350 mM Tris Base, 10% SDS, 6% BME, 30% glycerol, 0,012% BPB, pH 6,8) in 0,2 mL tubes, denatured at 100˚C/5 minutes and resolved on 4% stacking and 10% separating gel at 75 V and 150 V, respectively, in MightySmall II SE260 or SE640apparatus (Hoefer, San Francisco, CA, USA). Proteins were then transferred to methanol-activated PVDF membrane in semi-dry blotting apparatus PHERO-Multiblot (Biotec-Ficher, Reiskirchen, Germany) at 0.6 mA/cm2 for 60 minutes. Membrane was blocked in phosphate-buffered saline with 0.1% Tween 20 (PBST) and 5% BSA and probed with rabbit preprorenin (288-317) diluted 1:3000 in PBST with 0.1% BSA followed by HRP-conjugated Goat anti-Rabbit IgG (H+L) secondary antibody (Thermo Fisher Scientific, Prague, Czech Republic) at 1:10,000 dilution.

Membranes were incubated with Clarity™ Western ECL Substrate (Bio-Rad, Prague, Czech Republic) according to manufacturer's instructions. Signal was captured on CP-BU Medical X-ray blue film (Agfa) developed by Fomadent solution set (Foma Bohemia, Tisice-Chrast, Czech Republic). The tubulin protein was visualized by incubation with Mouse anti-Acetylated tubulin (T6793, Sigma Aldrich) at dilution

1:3000 in 0.1% BSA and 0.1% Tween 20 in PBS for 1 hour at RT, followed by incubation with Goat anti-Mouse HRP (Pierce) under conditions and using detection as described above.

Quantitative analysis of renin and prorenin by immunoradiometric assay (IRMA)

Cell lysate was prepared as described above. The medium was centrifuged at 15,000 x g for 10 min, and the resulting supernatant was mixed with protease inhibitor cocktail in ratio 100:1 (vol/vol).
For renin determination, 50 µl of the medium and 5 µl of the lysate were diluted to a final volume of 200µl with PBS. For trypsin-activated total renin and prorenin amount, 5µl of medium and 2.5µl of lysate were incubated at 37°C for 30 min in a 50µl PBS reaction containing 100 µg and 400 µg of trypsin, respectively. The reactions were stopped by 1µl of 10 mg/mL trypsin inhibitor (PMSF, Roche, Prague, Czech Republic) and diluted to a final volume of 200 µl with PBS.

Ten µl of the resulting mixtures was mixed with 290 µl of PBS and 100 µl of the anti-hRenin (I-125) reagent (Renin III Generation Kit, CISBIO Bioassays, France), and the renin amount was measured according to manufacturer's instructions.

Measurement of the enzymatic activity of renin secreted into the culture media

We measured the enzymatic activity of renin before and after cleavage of the propeptide region and of prorenin secreted into culture media after transient expression of renin variants and wild type renin. Seeding, maintaining and transfection were performed as described above. Twenty four hours after lipofection, the medium was collected and divided into 2 tubes. Trypsin / EDTA 1x (volume ratio medium : T/E = 1: 3) was added to one tube and incubated 30 min at 37°C for cleavage of prosegment from prorenin. The trypsin reaction was stopped by adding of 2,6 µL of 50mM PMSF (Roche) and incubated for 15 min at room temperature. 100µL media before and after trypsin incubation were placed into a

96-well plate and 50µL of 100x diluted renin substrate conjugated with 5-FAM and QXL520 was added (part of SensoLyte 520 Renin Assay Kit, AnaSpec, San Jose, CA). The fluorescent signal was monitored at 528 nm every 15 min for 3 hr at 37°C on an Infinite 2000Pro microplate reader (Tecan, Austria). Each sample either before or after trypsin activation was measured in triplicate. For graph construction, we used values after 75 minutes from the start of measurement, which was the time of maximum signal in linear part of enzymatic curves.

Confocal microscopy

1,5 x 10^5 HEK293 cells were plated on polysinated glass coverslips for 24 hours and transiently transfected by LipofectamineTM3000 with 1µg plasmid DNA of wt renin, L16del, C20R, L13Q, L16P, W17R, T26I, M39K, C325R, I366N, P8A, R33W, respectively according to the manufacturer's protocol. 24 hours after lipofection, cells were quickly washed with PBS1x and fixed with cold 100% methanol. After fixing, cells were washed three times in PBS 1x and proteins were blocked for 30 min at room temperature in PBS with 5% FCS. Cells were incubated over night at 4°C with rabbit primary antibody anti-human preprorenin 288-317 (Yanaihara) at a dilution of 1:50 or mouse anti-PDI (Enzo) at a dilution 1:200 or mouse anti-ERGIC (Acris) at a dilution 1:200. For colocalization with Golgi Apparatus we used mouse anti-GM130 (ab 169276, Abcam) at a dilution of 1:300. For colocalization with lysosomes we used mouse anti-LAMP2 (H4B4) (ab 25631, Abcam) at a dilution of 1:500. Cells were washed five times in PBS 1x and incubated with donkey anti-rabbit Alexa Fluor 555 and goat anti-mouse Alexa Fluor 488 (Invitrogen) at dilution 1:1000. All antibodies were diluted in PBS 1x with 5% FCS and 0.05% Tween 20. Cells were washed four times and mounted into Antifade with DAPI (Invitrogen) for confocal imaging.

Image acquisition and analysis

Prepared slides were analyzed by confocal microscopy. XYZ images were sampled according to Nyquist criterion using a LeicaSP8X laser scanning confocal microscope, HC PL APO objective (63x, N.A. 1.40),

405, 488 and 543 laser lines. Images were restored using a classic maximum likelihood restoration algorithm in the Huygens Professional Software (SVI, Hilversum, The Netherlands). The colocalization maps employing single pixel overlap coefficient values ranging from 0-1, were created and the colocalization coefficients were calculated in the Huygens Professional Software. The resulting overlap coefficient values are presented as the pseudo color which scale is shown in corresponding lookup tables (LUT). Approximately ten cells per variant were analyzed.

Supplementary References

S1. Zivna M, Hulkova H, Marignon M, et al. Dominant renin gene mutations associated with early- onset hyperuricemia, anemia, and CKD. *Am J Human Genet*. 2009;85:204-213

S2. Bleyer AJ, Zivna M, Hulkova H, et al. Clinical and molecular characterization of a family with a dominant renin gene mutation and response to treatment with fludrocortisone. *Clin Nephrol*. 2010;74:411-422

S3. Beck BB, Trachtman H, Gitman M, et al. Autosomal dominant mutation in the signal peptide of renin in a kindred with anemia, hyperuricemia, and CKD. *Am J Kidney Dis*. 2011;58:821-825.

S4. Clissold RL, Clarke HC, Spasic-Boskovic O, et al. Discovery of a novel dominant mutation in the REN gene after forty years of renal disease: a case report. *BMC Nephrol*. 2017;18:23

S5. Petrijan T, Menih M. Discovery of a Novel Mutation in the REN Gene in Patient With Chronic Progressive Kidney Disease of Unknown Etiology Presenting With Acute Spontaneous Carotid Artery Dissection. *J Stroke Cerebrovasc Dis*. 2019;28:104302.

S6. Abdelwahed M, Chaabouni Y, Michel-Calemard L, et al. A novel disease-causing mutation in the Renin gene in a Tunisian family with autosomal dominant tubulointerstitial kidney disease. *Int J Biochem Cell Biol*. 2019;117:105625.

S7. Schaeffer C, Izzi C, Vettori A, et al. Autosomal Dominant Tubulointerstitial Kidney Disease with Adult Onset due to a Novel Renin Mutation Mapping in the Mature Protein. *Sci Rep*. 2019;9:11601.